Quantifying probabilities of volcanic events: The example of volcanic hazard at Mount Vesuvius

Warner Marzocchi,[1] Laura Sandri,[1] Paolo Gasparini,[2] Christopher Newhall,[3] and Enzo Boschi[4]

Received 26 April 2004; revised 21 July 2004; accepted 17 August 2004; published 9 November 2004.

[1] We describe an event tree scheme to quantitatively estimate both long- and short-term volcanic hazard. The procedure is based on a Bayesian approach that produces a probability estimation of any possible event in which we are interested and can make use of all available information including theoretical models, historical and geological data, and monitoring observations. The main steps in the procedure are (1) to estimate an a priori probability distribution based upon theoretical knowledge, (2) to modify that using past data, and (3) to modify it further using current monitoring data. The scheme allows epistemic and aleatoric uncertainties to be dealt with in a formal way, through estimation of probability distributions at each node of the event tree. We then describe an application of the method to the case of Mount Vesuvius. Although the primary intent of the example is to illustrate the methodology, one result of this application merits special mention. The present emergency response plan for Mount Vesuvius is referenced to a maximum expected event (MEE), the largest out of all the possible eruptions within the next few decades. Our calculation suggest that there is a nonnegligible (1–20%) chance that the next eruption could be larger than that stipulated in the present MEE. The methodology allows all assumptions and thresholds to be clearly identified and provides a rational means for their revision if new data or information are obtained. *INDEX TERMS:* 8414 Volcanology: Eruption mechanisms; 6309 Policy Sciences: Decision making under uncertainty; *KEYWORDS:* volcanic hazard, forecasting eruptions, Mount Vesuvius

Citation: Marzocchi, W., L. Sandri, P. Gasparini, C. Newhall, and E. Boschi (2004), Quantifying probabilities of volcanic events: The example of volcanic hazard at Mount Vesuvius, *J. Geophys. Res.*, *109*, B11201, doi:10.1029/2004JB003155.

1. Introduction

[2] The hazard and risk assessment of volcanoes located near urbanized areas is one of the main goals of modern volcanology, as population density around some active volcanoes has grown rapidly in the last century. Volcanic risk is usually defined as [e.g., *UNESCO*, 1972; *Fournier d'Albe*, 1979]

$$\text{risk} = \text{hazard} \times \text{value} \times \text{vulnerability} \qquad (1)$$

where hazard is the probability of any particular area being affected by a destructive volcanic event within a given period of time; the value is the number of human lives at stake, or the capital value (land, buildings, etc.), or the productive capacity (factories, power plants, highways, etc.) exposed to the destructive events; the vulnerability is a measure of the proportion of the value which is likely to be lost as a result of a given event.

[3] Equation (1) represents a very general framework to assess quantitatively the risk for any kind of natural destructive event. The strategy to evaluate each of the parameters involved is generally different according to the type of event we are considering: a volcanic eruption can produce different forms of destructive event, such as pyroclastic and lava flows, tephra, lahars, gas emission, ground deformation, volcano-seismic events, and so on. Compared to the case of earthquakes, where the main hazard can be defined in terms of ground shaking only (even though ground rupture and liquefaction can be locally relevant), volcanic hazard in a given area is the summation of different destructive effects, such as horizontal pressures and temperatures of pyroclastic and lava flows, vertical load of ash fall, and ground shaking due to seismic activity.

[4] Volcanic hazard is difficult to quantify because of the intrinsic complexity of the eruptive processes and the paucity of past data. In principle, we may estimate the volcanic hazard in a similar way to seismology, where the hazard is usually calculated by modeling statistically the past earthquakes that have occurred in the region being studied. However, in volcanology there are important differences that have to be taken into account: first, as mentioned

[1] Istituto Nazionale di Geofisica e Vulcanologia-Bologna, Bologna, Italy.
[2] Dipartimento di Fisica, Universita di Napoli "Federico II," Naples, Italy.
[3] U.S. Geological Survey, University of Washington, Seattle, Washington, USA.
[4] Istituto Nazionale di Geofisica e Vulcanologia-Roma, Rome, Italy.

0148-0227/04/2004JB003155$09.00

above, violent eruptions are relatively rare events (on the human timescale), implying that the observational data are often insufficient to build a reliable and robust statistical model; second, data from monitoring of volcanoes can help with mid- to short-term (few years to minutes) term forecasting. The last point is very important. The hazard estimated only from past data is relevant over long timescale (years to decades). Such a long-term volcanic hazard assessment allows different kinds of hazards (volcanic, seismic, industrial, floods, etc.) in the same area to be compared, which is very useful for cost/benefit analysis of risk mitigation actions, and for appropriate land use planning and location of settlements. In contrast, monitoring on mid to short timescales assists with actions for immediate vulnerability (and risk) reduction, for instance through evacuation of people from danger areas [e.g., *Fournier d'Albe*, 1979].

[5] Most recent hazard studies reported in the scientific literature depict only certain specific aspects of the volcanic hazard, for instance, mapping the effects on the territory of a single eruptive phenomenon (e.g., a lava flow, pyroclastic flow, lahar) for a specific type of eruption [e.g., *Esposti Ongaro et al.*, 2002; *Cioni et al.*, 2003]. While useful in themselves, such maps based on specific events would be of much greater value if they were accompanied by statistical estimation of the probability of occurrence of the eruptive event and/or the phenomenon considered, so that quantitative probabilistic estimates may be made of the long-term hazard. In some cases, the probability of long-term occurrence of some specific eruptive episode is calculated by assuming (more or less explicitly) a Poisson process [e.g., *Scandone et al.*, 1993a; *Lirer et al.*, 2001]; this hypothesis, however, is still a matter of debate [e.g., *Gusev et al.*, 2003] because it makes the presumption that the next eruption is independent of the time and size of the last eruption.

[6] Most recent research on the short-term hazard (mid- to short-term forecasting) is based on a deterministic approach [e.g., *Voight and Cornelius*, 1991; *Kilburn*, 2003; see also *Hill et al.*, 2001]. The alternative approach is probabilistic (e.g., *Newhall and Hoblitt* [2002] (hereinafter referred to as NH02) and *Aspinall and Woo* [1994]). NH02 propose an event tree scheme to estimate the probability of all the relevant possible outcomes of a volcanic crisis and, in general, to quantify the volcanic hazard and risk.

[7] In this paper we implement such an event tree scheme in a formal quantitative way and apply it to volcanic hazard at Mount Vesuvius, the volcano with one of the highest levels of risk in the world. A Bayesian approach is used at different levels of the model, and it is fundamental in many aspects. Besides combining the probabilities at the nodes of the tree [see NH02], the Bayesian approach allows merging theoretical models of the eruptive process, past (historical and geological) data, and data from monitoring of the volcano. Thus it allows aleatoric and epistemic uncertainties of the model to be dealt with in a formal way, and all to be accommodated in a hazard or risk assessment.

[8] The concept of aleatoric (stochastic) and epistemic (data or knowledge limited) uncertainties is of primary importance in hazard/risk studies [see, e.g., *Woo*, 1999]. The aleatoric uncertainty is associated with the impossibility of predicting deterministically the evolution of a system due to its intrinsic complexity. The epistemic uncertainty is associated with limitations in our knowledge of the system. In general, the first one produces an irreducible stochasticity (randomness) in outcomes, regardless our physical knowledge of the system; the second one is, in principle, reducible, by increasing the number or quality of data and/or the knowledge of the physical system (for more details, see Appendix A).

[9] Another reason for the Bayesian approach is philosophical. It might be argued that the scarce number of past data and the relatively poor knowledge of the preeruptive physical processes do not allow solution of the hazard/risk problem from a rigorous scientific point of view, i.e., to build a useful and testable model. On the other hand, the extreme risk pushes us to be pragmatic and attempt to solve the problem from an "engineering" point of view: by this, we mean that the devastating potential of explosive volcanoes close to urbanized areas forces the scientific community to address the issue as precisely as possible. This is best done by treating scientific uncertainty in a fully structured manner and, in this respect, Bayesian statistics is a suitable framework for producing a volcanic hazard/risk assessments in a rational, probabilistic form [e.g., *UNESCO*, 1972; *Gelman et al.*, 1995].

[10] The paper is composed of two parts. In the first methodological part we describe the event tree scheme and the innovative quantitative approach used to calculate the probability at each node and, consequently, for each possible event. In the second part, we provide an application of the method to define the hazard at Mount Vesuvius. Mount Vesuvius is located in a densely urbanized area with more than 700,000 people living on the flanks of the volcano. The enormous social and economic impact of a reactivation of the volcano demands a volcanic hazard assessment that is as well constrained and meaningful as possible. By way of example, in section 3 we illustrate how the event tree scheme might be used in a hypothetical future scenario as it evolves at this volcano.

2. Event Tree Scheme

2.1. Structure of the Event Tree

[11] The main advantages of the event tree (ET) scheme consist of its intrinsic simplicity and its capacity for providing a quantitative estimation of any kind of volcanic hazard and individual risk. A detailed description of a generic volcano ET can be found in NH02. Here, we briefly summarize the main points and focus our attention on the estimation of the probability at each node.

[12] The ET is a tree graph representation of events in which individual branches are alternative steps from a general prior event, state, or condition through increasingly specific subsequent events (intermediate outcomes) to final outcomes. In this way, an ET shows all relevant possible outcomes of volcanic unrest at progressively higher degrees of detail. The branches at each node point to different possible events, although these need not be mutually exclusive or exhaustive. In Figure 1, we report a general ET for an explosive volcano (see, e.g., NH02). At successive nodes, we estimate the probability density function (PDF) of the probability (for more details, see below) for the following states: node 1, $p(\theta_1)$, unrest occurs within a given time interval (τ); node 2, $p(\theta_2)$, the unrest is due to

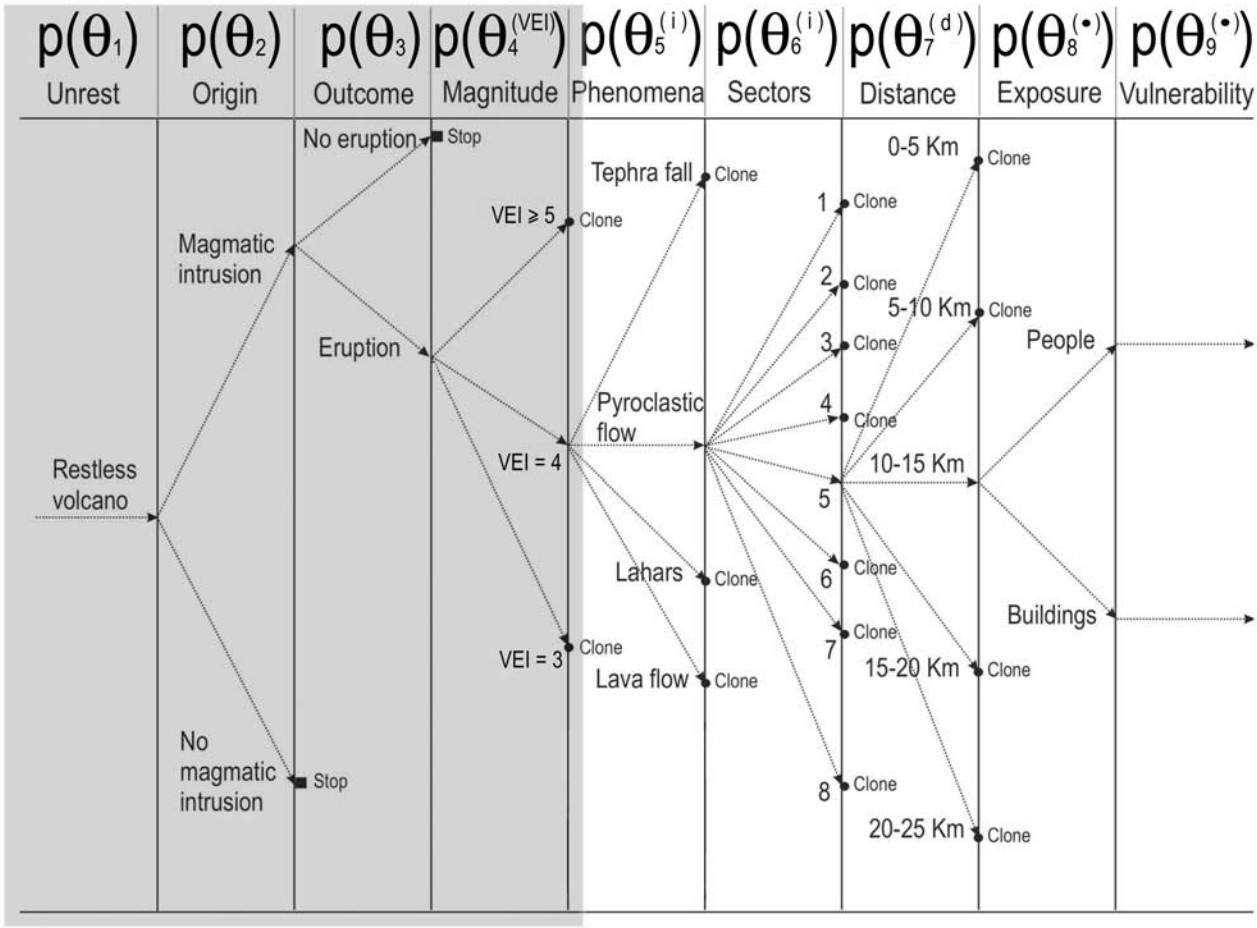

Figure 1. Sketch of the event tree for Mount Vesuvius. The nine steps of estimation progress from general to more specific events, as described in the text. Note that any branch that terminates with Clone is identical to the subsequent central branch. For example, in the ''sectors'' column, the clones relative to sectors 1, 2, 3, 4, 6, 7, and 8 are identical to the central branch relative to sector 5. The branches terminating with ''stop'' are not discussed here because they cannot develop into very dangerous subsequent events. The shaded part of ET is the one considered in the application to Mount Vesuvius.

magma, and given unrest is detected; node 3, $p(\theta_3)$, the magma will reach the surface (i.e., it will erupt) in a given time interval (τ), provided that the unrest has a magmatic origin; node 4, $p(\theta_4^{(VEI)})$, the eruption will be of a certain magnitude (VEI), provided that there is an eruption; node 5, $p(\theta_5^{(j)})$, a certain jth phenomenon (lava flow, tephra fall, pyroclastic flow, lahar, etc.) will occur, provided that the magnitude of the eruption is of a certain value; node 6, $p(\theta_6^{(j)})$, the phenomenon will move into the jth specific sector, given that the phenomenon has occurred; node 7, $p(\theta_7^{(d)})$, the phenomenon will reach a certain distance d from the vent, provided that the phenomenon has occurred and moved into a certain (usually radial) sector; node 8, $p(\theta_8^{(\cdot)})$, an individual or a building will be present at the specified sector and distance from the vent reached by phenomenon (this is called exposure); and node 9, $p(\theta_9^{(\cdot)})$, a hypothetical individual will be killed (or injured) or a building will be destroyed (or damaged) at the specified sector and distance from the vent, given that the phenomenon arrives there and that person and/or building is present (this is called vulnerability; see equation (1)). The knowledge of the PDF at the nodes allows the probability of any desired event to be estimated through the use of classical probability theorems [cf. *Aspinall et al.*, 2003].

[13] Figure 1 highlights another very appealing feature of the ET, that is, the formulation provides a powerful scheme able to integrate the results from different studies which may focus on different aspects of the hazard/risk problem. For instance, the so-called hazard maps of the effects of a well defined phenomenon based on some selected similar eruptions [e.g., *Cioni et al.*, 2003] do not represent the ''absolute'' magnitude of the hazard, but the hazard conditional on the occurrence of a specific event (i.e., they represent the nodes 6 and 7). From Figure 1, we can see that the knowledge of the first 4 nodes allows us to define quantitatively the probabilities of a volcanic eruption of any magnitude in a given time interval (also called source hazard). Including the subsequent node, we have the hazards of single well defined phenomena (the occurrence of a pyroclastic flow, tephra, lahars, etc.). The first node is particularly important: depending on its value (if we are in a quiet period, or during unrest), we can proceed to estimate either the long-term or short-term hazard (see below).

[14] From a practical point of view, we need to find ways to estimate or determine the PDF at each node. Here, and in the application to Mount Vesuvius described below, we estimate the PDF of the first four nodes (necessary to define the source hazard; see above) by taking into account three types of data: (1) a priori and theoretical beliefs, (2) historical and geological data from the volcano and from similar volcanoes (henceforth called "analogs"), and (3) new measurements taken at the volcano (monitoring). Even though we consider only the first four nodes of the ET, the strategy adopted can be generalized to apply to the subsequent nodes.

2.2. Estimating the Probability at the Nodes

[15] Here, we propose a Bayesian strategy for estimating the probability at each node. This improves upon NH02 by including a formal probabilistic treatment of the available data and their uncertainties (aleatoric and epistemic; see Appendix A). The treatment and estimation of the uncertainties are very important for correctly interpreting the results and to guide future researches on this topic (see below).

[16] Estimating a value for a probability always involves a subjective element (even with copious data in the frequentist approach). In most of the cases, in fact, we have to estimate such probabilities from few data, theoretical (often untested) beliefs, and/or models. For these reasons, we follow a fully Bayesian approach and associate with each event of a node a probability distribution rather than a single value as in NH02. That is, we estimate uncertainties on these event probabilities (sometimes, "probabilities of probabilities" [see, e.g., *Woo*, 1999]). In this way, we can also formally account for any kind of uncertainty associated with the probability of each node that, in this case, is a random variable. Some comments on notation are needed at this point: $\theta_k^{(j)}$ is the random variable reporting the probability of the jth event at the kth node. For the nodes characterized by a binary type of event (i.e., unrest or not, magma or not, eruption or not; see Figure 1) we drop the upper index (j). To avoid the use of a cumbersome notation, in the following, we use the upper index (j) only if strictly necessary. The function $p(\theta_k)$ represents the probability density function (PDF) of the random variable θ_k.

[17] The distribution $p(\theta_k)$ has to be unimodal and with domain [0,1] because the random variable is a probability. A suitable distribution with these requirements is the Beta distribution described in Appendix A. The key point of our strategy is that the available empirical and theoretical information modify the mean and variance (see equations (A5) and (A6) in Appendix A), and therefore the probability distribution. In general, all the available information determines the mean of the distribution (aleatoric uncertainty), while the variance of the distribution (epistemic uncertainty) is modified (usually significantly reduced) by having more available data. The PDF associated with θ_k is calculated by following three steps.

[18] In step a we define the initial distribution as $p_a(\theta_k)$ that takes into account our a priori theoretical beliefs.

[19] In step b we define $p_b(\theta_k)$ as $p_a(\theta_k)$ modified by including past data (from the volcano in question and from its analogs) by using Bayes' theorem.

[20] In step c we define $p_c(\theta_k)$ as $p_b(\theta_k)$ modified by including fresh measurements from current monitoring, again by using Bayes' rule.

[21] Steps a and b are based on common procedures of analysis in the Bayesian statistical approach [e.g., *Gelman et al.*, 1995]. Step c contains the largest part of subjectivity and includes the volcanological model used; here, the monitoring data are used for two different purposes: to detect unrest and to modify estimates of the mid- to short-term hazard (few years to minutes) during unrest.

2.2.1. Step a

[22] The initial probability distribution at each node is based on the a priori and theoretical beliefs and/or models. If we do not have any a priori or theoretical information, we have to assume complete ignorance of the probability distribution at the considered node. This is accomplished by using a uniform distribution

$$p_a(\theta_k) = 1 \qquad \forall \quad \theta_k \in [0,1] \tag{2}$$

(Beta distribution with $\alpha_a = \beta_a = 1$). If we have some a priori or theoretical information, this can be used to define the distribution depending upon its reliability: thus $p_a(\theta_k)$ can assume a different form depending on the model assumed. For instance, if we assume the presence of a complex system at the kth node [e.g., *Bak et al. 1988*], it may be appropriate to use a Beta distribution for each probability θ_k ($p_a(\theta_k)$) centered around the average calculated through a power law distribution. We discuss this point in more detail in section 3.

2.2.2. Step b

[23] In step b, $p_a(\theta_k)$ is combined with past data through the Bayes' theorem [cf. *Aspinall et al.*, 2003]. In particular, we model the information provided by past data, in the nodes where they are available. Let us consider, for the sake of example, a very common case: by means of a Bernoulli trial scheme we can account for past data to obtain the so-called likelihood:

$$p(n \mid \theta_k) = \binom{N}{n} \theta_k^n (1-\theta_k)^{N-n} \tag{3}$$

where N is the total number of trials or cases available and n is the number of "successes" among these cases. Then $p_b(\theta_k)$ is defined through the Bayes theorem

$$p_b(\theta_k) \equiv p(\theta_k \mid n) = \frac{p_a(\theta_k) p(n \mid \theta_k)}{p(n)} \tag{4}$$

[24] If $p_a(\theta_k)$ has a uniform distribution (state of maximum ignorance), we have

$$\begin{aligned} p_b(\theta_k) &= (N+1)\frac{N!}{(N-n)!n!}\theta_k^n(1-\theta_k)^{N-n} \\ &= \frac{\Gamma(N+2)}{\Gamma(n+1)\Gamma(N-n+1)}\theta_k^n(1-\theta_k)^{N-n} \\ &= \mathrm{Beta}(\alpha_b = n+1, \beta_b = N-n+1) \end{aligned} \tag{5}$$

while in the more general case where $p_a(\theta_k) = \mathrm{Beta}(\alpha_a, \beta_a)$, we have

$$p_b(\theta_k) = \mathrm{Beta}(\alpha_b = n + \alpha_a, \beta_b = N - n + \beta_a) \tag{6}$$

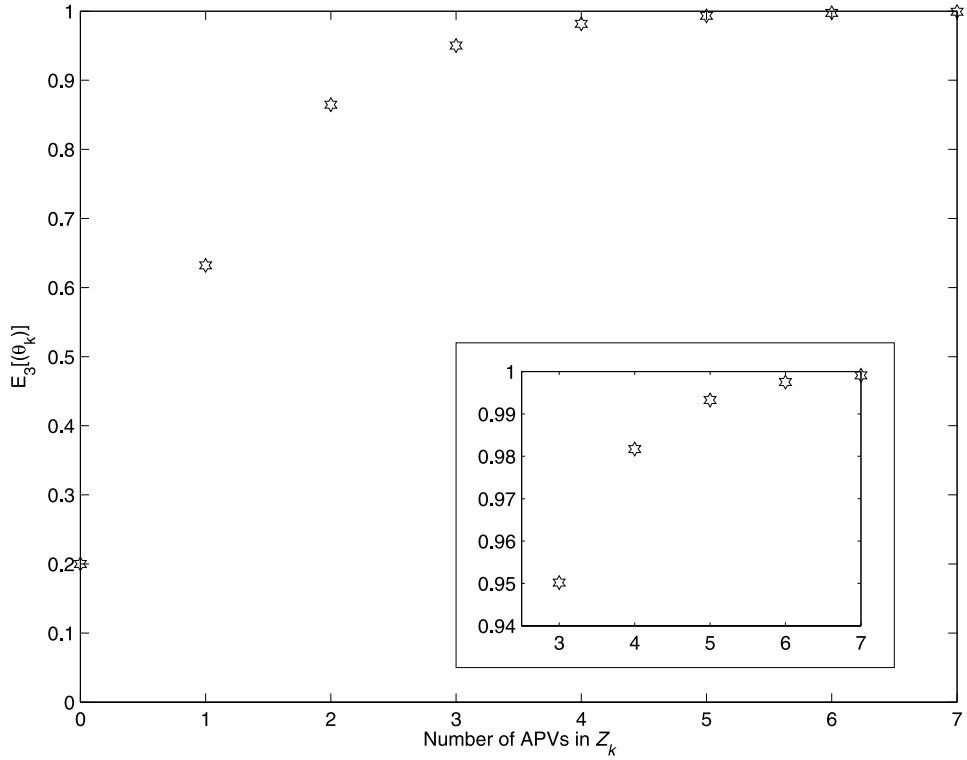

Figure 2. Example of $E_c[\theta_k]$ as a function of the number of APVs in Z_k for the second and third nodes (see equation (8)). Here, the average when no APVs are observed is arbitrarily set to 0.2.

[25] The first two moments of $p_b(\theta_k)$ are determined by equations (A5) and (A6), respectively (see Appendix A), with α_b and β_b. In the case where no past data are available, $p_b(\theta_k) = p_a(\theta_k) = \text{Beta}(1,1)$, corresponding to a uniform distribution (see Appendix A).

2.2.3. Step c

[26] Step c involves the largest part of the subjectivity introduced in this approach. Monitoring data are not always available for periods before past eruptions, especially at explosive volcanoes that erupt infrequently. At the same time, it is obvious that monitoring data contain fundamental information that must be used.

[27] The key point of this step is that monitoring data are used to detect unrest and to modify the first moment (the mean) of $p_b(\theta_k)$ during unrest. In other words, in a "quiet" period of the volcano, monitoring is used only to watch for unrest. When unrest is detected, the data obtained can then be used to modify the probability of mid- to short-term hazard at the relevant nodes.

[28] In order to implement the updating of each node k with new information from monitoring, a certain number of parameters (M_k) and relative thresholds (T_j; $j = 1,\ldots, M_k$) are selected to describe the state of the system at time t by means of the time series $Z_k(t)$:

$$Z_k(t) = \omega_1 z_1(t) + \ldots + \omega_{M_k} z_{M_k}(t) \tag{7}$$

where $z_i(t) = 1$ if measurement $i \geq (\leq)\ T_i$ at time t and $z_i(t) = 0$ otherwise; $\omega_i \geq 1$ is the (integer) weight for measurement i. Any $z_i(t) = 1$ is called anomalous parameter value (APV). Note that consistency requires that an APV in a generic kth node implies the existence of at least one APV also in each previous node. The quantity $Z_k(t)$ can be viewed as a characterization of the preeruptive state of the volcano at the time t and is now used to modify $p_b(\theta_k)$ into $p_c(\theta_k)$. For the sake of conciseness, hereinafter we consider $Z_k \equiv Z_k(t)$, and $z_i \equiv z_i(t)$.

[29] The specific way in which Z_k modifies $p_b(\theta_k)$ depends on the node considered. For the first node, the existence of an APV means the presence of unrest, therefore $p_c(\theta_1)$ becomes a Dirac's δ distribution centered around 1. That is, the existence of even one APV raises the probability of unrest to 1, by definition. For the second and third nodes, a large number of APVs results in a higher average probability. The largest increase in average probability occurs when we observe the first APV (see Figure 2):

$$E_c[\theta_k] = \begin{cases} \frac{E_b[\theta_k]}{\psi} & \text{if} \quad Z_k = 0 \quad \text{at time } t \\ 1 - \exp^{-Z_k} & \text{if} \quad Z_k > 0 \quad \text{at time } t \end{cases} \tag{8}$$

where $E_c[\theta_k]$ is the average of the Beta distribution (see Appendix A and equations (A5) and (A6)) and ψ is a factor that considers the reduction of the average probability when we observe no APVs. Equation (8) also tells that during unrest any APVs defines the new average probability neglecting theoretical and past information used in the previous steps.

[30] For the second and third nodes, usually both $p_b(\theta_k)$ and $p_c(\theta_k)$ have a Beta distribution. This means that, for example,

$$E_c[\theta_k] = \frac{\alpha_c}{\alpha_c + \beta_c} \tag{9}$$

The sum $\alpha_b + \beta_b = \alpha_c + \beta_c$ is related only to the number of data upon which $p_b(\theta_k)$ has been defined (see Appendix A). This means that monitoring results modify mainly the mean of the Beta distribution because the variance can only be reduced by having more data on volcano's past.

[31] Despite the apparent arbitrariness of this method of combining new monitoring data with past data and theoretical models, the proposed tool has two important advantages: (1) there is reduced subjectivity of approach compared to the common case where no consistent rules for hazard assessment are defined and (2) the procedure can highlight "weak" points of our knowledge of preeruptive processes (where epistemic uncertainty is large). The latter attribute can be used to focus the objectives of future studies.

3. Assessment of Eruption Probabilities at Mount Vesuvius

[32] Mount Vesuvius is located in a densely populated area with millions of people living on its flanks and in the immediate vicinity of the volcano. In the past, Mount Vesuvius produced several large explosive eruptions that devastated the surrounding area. It last erupted in 1944 with a VEI = 3 weakly explosive event that sent lava flows into the nearest part of the town of S. Sebastiano. There were about 40 fatalities [see *Scandone et al.*, 1993b]. Prominent previous eruptions were VEI = 4 events in 472 A.D. and 1631 [see, i.e., *Scandone et al.*, 1993b], preceded by the well-known Pompeii eruption in 79 A.D. Mount Vesuvius shows decades to centuries of frequent small eruptions (open vent behavior) and a few long reposes followed by large explosive eruptions (closed vent behavior). Open vent behavior prevailed through the early 20th century until 1944. Since 1944, however, an unusually long repose (60 years and continuing) suggests this volcano may now be in a closed vent condition.

[33] Unfortunately, very little is known of precursors to large eruptions that follow long reposes. For the 79 A.D. eruption the sum total of that knowledge is summarized by *Gigante* [1991, p. 159]. Pliny the Younger, in his second letter, states that

> before [the 79 A.D. eruption], the earth had been shaken for several days but we were not much scared because earthquakes are frequent in Campania.

The excavations in Pompeii and Herculaneum indicate that many public edifices and private houses were under repair, a fact which confirms the statement by Pliny. Giulio Cesare Recupito and Giulio Cesare Braccini are two scholars who witnessed and described in great detail the 1631 eruption [*Recupito*, 1632, p. 59; see also *Nazzaro*, 1998]. Recupito states that people living in villages on the slopes of Mount Vesuvius

> since December 10 (six days before the onset of the eruptions) slept badly because of subterraneous rumbles... Some of them who ascended the mountain felt a continuous tremor... Other inhabitants observed that water in the wells had become dirty, without any rain, and some wells were dry. If they had been wise from this, even if not from others, they could have foreseen the earthquakes which followed and be saved. However, as someone said *perituri non recipient consilia* (those whose destiny is death do not accept any advice).

Braccini reports that several reliable people had descended inside the summit crater about 1 month before the eruption. They returned to the summit crater after 15 days finding that the bottom had uplifted so much that it was possible to walk through the crater.

[34] Mount Vesuvius is a good example of how risk can increase dramatically in a short time because value and vulnerability increase much faster than hazard. In 1944, about 300,000 people were living on its slopes. That population has more than doubled and some towns have expanded to within 2–3 km of its central crater. Critical buildings such as schools and hospitals have been built very close to fracture zones on the volcano's slopes where in recent centuries eruptive vents opened.

[35] Civil administrators are becoming conscious that in these conditions, an event even smaller than the 1944 eruption can be catastrophic from an economic and social point of view. For implementation of mitigation actions and for land use planning they need quantitative assessments of volcanic hazard. As mentioned in the introduction, this would allow (1) a comparison of volcanic hazards with other natural and anthropogenic hazards existing in the same area for cost/benefit analysis of risk mitigation actions and (2) the preparation of adequate crisis management plans which consider the different probabilities of possible eruptive scenarios, and the variations that can occur a short time before onset and during the evolution of an eruptive crisis.

[36] Until now, the absolute level of volcanic hazard at Mount Vesuvius is unknown. Most recent efforts have been devoted to estimation of the potential spatial distributions of pyroclastic flows and tephra falls based on past eruptions and numerical simulations [*Barberi et al.*, 1990; *Esposti Ongaro et al.*, 2002; *Cioni et al.*, 2003]. These estimations assume the occurrence of a "maximum expected event (MEE)", the largest out of all the possible eruptions in the next few decades [cf. *Barberi et al.*, 1990; *Cioni et al.*, 2003]. The MEE used as the basis for the present emergency plan for Mount Vesuvius is a VEI = 4 eruption, similar to those of 472 A.D. and 1631 [see, *Scandone et al.*, 1993b].

[37] The MEE concept considers repose intervals, but assumes that magma supply remains more or less constant at timescales of decades, and that (as a maximum) the volume of the next eruption will not exceed the volume of magma accumulated since the last eruption [*Santacroce*, 1983]. However, we now know that the second of these is inconsistent with (1) evidence from the TOMOVES project (Mount Vesuvius tomography [*Capuano et al.*, 2003]) that present-day magma bodies are considerably larger than the volumes of most recent eruptions and (2) historical examples of some large explosive eruptions that have occurred after just a few years of repose. For instance, the Mount St. Helens 1482 event followed another VEI = 5 eruption in 1480 and was the fourth in a series of five Plinian events that occurred over just a few years; other examples come from Taal 1754, Asama 1783, Mayon 1814 and 1897, Cotopaxi 1877, and Quizapu 1932 (phreatic eruptions from 1903 to late 1920s, mafic Strombolian eruptions from 1926 to 1932, and a large VEI = 5 silicic eruption 1932). Krakatau 1883 could also be included here because, even though its preceding repose was about 200 years, much more time would have been required to supply the 13 km^3 of magma that was erupted. However, we show in this paper

Table 1. Node 1: Monitoring Parameters and Their Threshold to Define Unrest

Parameter	Threshold	Basis
$z_{n_e} = 1$	$n_e \geq 100$ month^{-1}	last 32 years data [*Zollo et al.*, 2002]
$z_{M_d} = 1$	$M_d \geq 4.1$	last 32 years data [*Zollo et al.*, 2002]
$z_{n_{LF}} = 1$	$n_{LF} \geq 3$ month^{-1} (depth ≥ 1 km)	swarm of LF never recorded
$z_{\Pi_{SO_2}} = 1$	$\Pi_{SO_2} = 1$	no SO_2 in the fumaroles in recent years
$z_{\Phi_{CO_2}} = 1$	$\Phi_{CO_2} \geq 5$ kg m^{-2} d^{-1}	2 times the average in the last 3 years [*Granieri et al.*, 2003]
$z_{\dot{\varepsilon}} = 1$	$\dot{\varepsilon} > 0$ d^{-1}	inflation never recorded
$z_T = 1$	$T > 105$°C	10% higher than observations since 1990 [*Chiodini et al.*, 2001]

that there is a nonnegligible probability that the next eruption of Mount Vesuvius will be larger than the present MEE.

3.1. Structure of the Event Tree at Mount Vesuvius

[38] In order to define the ET at Mount Vesuvius, the first step is to define its general structure. For this purpose, we think that the ET shown in Figure 1 is suitable also for Mount Vesuvius. Here, we focus our attention on the estimation of the probabilities for the first 4 nodes that define the hazard of a specific eruption at Mount Vesuvius. Before defining the probability at each node, it is useful to summarize the available information.

[39] In step a (see section 2.2.1) the a priori and theoretical beliefs can be represented either by a priori assumptions or by a maximum ignorance state.

[40] In step b (see section 2.2.2) the past (historical) data can be in the form of statistical distribution of past data or of observed past frequencies. The type of data can be further divided into three categories: (1) past data from Mount Vesuvius, including limited qualitative information about precursors to the large 79 and 1631 eruptions; (2) data coming from analogs; and (3) data from worldwide volcanoes.

[41] In step c (see section 2.2.3) we make use of new measurements taken at Mount Vesuvius from routine monitoring taking into account the experience gained from other explosive volcanoes and on the availability of observables monitored almost continuously at Mount Vesuvius; in particular, we make use of three different measurements: seismic, in particular the monthly number of events, their magnitude distribution, their average frequency content and their focal depth; deformation, in particular strain rate and cumulative strain; temperature of the fumaroles; and gases emissions.

3.2. Estimating the Probability at the Nodes

[42] We will now describe, for each node k, how to compute the probability distributions $p_a(\theta_k)$, $p_b(\theta_k)$, and $p_c(\theta_k)$. Before going into the details of the calculations, we remark that the parameters and thresholds adopted here are relatively crude compared to the present state of monitoring at Mount Vesuvius, where sophisticated and detailed observations are regularly collected. For practical purposes, however, we think that our still scarce level of knowledge about preeruptive processes requires much care in using conceptual models, which certainly may aid interpretations of monitoring data but might also introduce unknown bias into the probability estimations.

[43] The set of parameters and thresholds adopted here have to be considered as representative only of the present state of the volcano (and this volcano in particular). Indeed, the volcano is an evolving system (in timescale of decades); therefore it is expected that some of the thresholds adopted here may need to be varied with time. Obviously, any future improvement in knowledge based on theory and/or phenomenological data can be used to modify the volcanological model (i.e., Z_k) and therefore the parameters that are taken into account and their chosen thresholds.

[44] Finally, we remind readers that the probabilities θ_1 and θ_3 depend on the time interval being considered. Here, we define this time interval $\tau = 1$ month. The choice of a 1 month time window is a practical one, approximating the longest lead times of precursors (see below), while being roughly twice the time needed for an evacuation. In general, alternative values of τ simply act on the relevant probabilities through a multiplicative factor.

3.2.1. Node 1 (Unrest): $p(\theta_1)$

[45] To estimate the probability at this node, we must first define what unrest is. This choice is unavoidably subjective, as is the choice of the parameters used to define it. We define unrest by using the monitoring information recorded at Mount Vesuvius since 1972, when the first seismometer that is still operating was installed.

[46] First, we list the seven parameters used to indicate unrest, and then we go on to define and discuss them:

- n_e number of seismic events per month with $M_d \geq 1.9$ recorded at the OVO station;
- M_d largest duration magnitude of the earthquakes recorded at the OVO station;
- n_{LF} number of low-frequency (LF) events per month;
- Π_{SO_2} presence of significant SO_2 (0, no; 1, yes);
- Φ_{CO_2} daily CO_2 emission rate;
- $\dot{\varepsilon}$ strain rate (inflation);
- T temperature of the fumaroles inside the crater.

[47] Formally speaking, equation (7) is written as

$$Z_1 = z_{n_e} + z_{M_d} + z_{n_{LF}} + z_{\Pi_{SO_2}} + z_{\phi_{CO_2}} + z_{\dot{\varepsilon}} + z_T \qquad (10)$$

and $\omega_i = 1$ for $i = 1, \ldots, 7$ (the parameters have the same weight).

[48] In Table 1 we report the parameters and thresholds. In general, if $Z_1 > 0$ (see equation (7)), unrest is occurring. In practice, this means that a single anomaly in any one of the parameters (a single APV) is sufficient to define unrest. Thus the choice of the thresholds requires careful consideration.

[49] We take $n_e \geq 100$ month^{-1}, obtained by considering all the seismicity recorded at OVO since 1972 with $M_d \geq 1.9$ as "background" seismicity [*Zollo et al.*, 2002; see also *De Natale et al.*, 2000]. The threshold is chosen by simulating random sampling from the generalized Poisson distribution given by *Zollo et al.* [2002] (see also Figure 3)

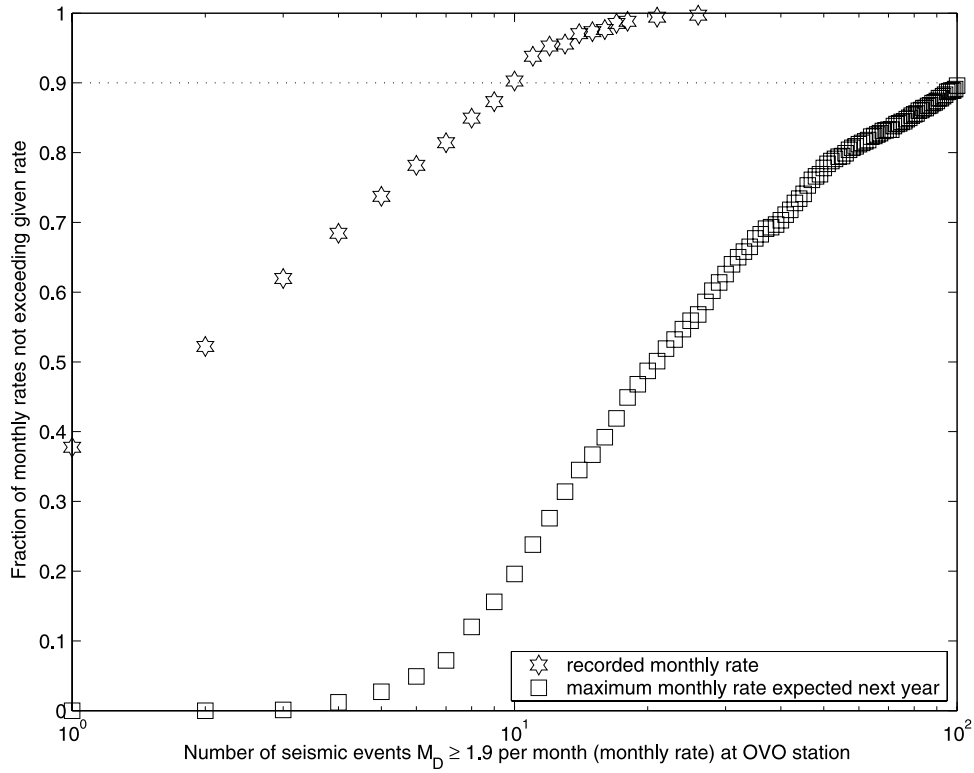

Figure 3. Empirical cumulative distributions of the monthly number of seismic events with $M_d \geq 1.9$ recorded at OVO station, and of the maximum monthly number of events expected for the next year at OVO station (see text for more details).

and collecting the maximum values for a time interval of 1 year. The threshold $n_e = 100$ month^{-1} is around the 90th percentile of the empirical distribution of the maximum values collected.

[50] For the magnitude M_d threshold, we assume that the distribution of the energy released and of the magnitude of the earthquakes since 1972 recorded at the OVO station represents the background activity. In particular, the magnitude of an individual event can be considered as a random variable from a power law distribution [e.g., *Aki*, 1965]. As before, we simulate random sampling from this distribution with a b value equal to 1.2 (a recent estimate for Mount Vesuvius is 1.2 ± 0.4 [see *Del Pezzo et al.*, 2003]), and we obtain the empirical distribution of the expected maximum magnitudes for the next year. The threshold $M_d = 4.1$ is the 90th percentile of such a distribution.

[51] LF events are usually inferred to be due to the presence of fluids, magmatic and/or hydrothermal [e.g., *Chouet*, 1996; *Neuberg*, 2000; *Chouet et al.*, 1994]. A small swarm of LF events would be taken to be indicative of unrest ($n_{\mathrm{LF}} \geq 3$ month^{-1}) because only sporadic and temporally isolated LF events have been recorded at Mount Vesuvius since it was continuously monitored (E. Del Pezzo and M. Martini, personal communication, 2004). Here, we consider only a swarm of low-frequency events occurring at a depth >1 km is potentially indicative of the presence of rising magma.

[52] Another parameter is the presence of a "significant" amount of SO_2 (yes/no). At present, acid gases like SO_2 are practically absent in the fumarolic fluids of the crater of Mount Vesuvius [*Chiodini et al.*, 2001]. The threshold of CO_2 emission rate is based on continuous monitoring at a single station inside the crater that measures the CO_2 flux in a very small area [*Granieri et al.*, 2003]. In almost 3 years of monitoring, the flux has an almost constant average of 2–3 kg m^{-2} d^{-1}. In this time period, two anomalous peaks of 5 and 20 kg m^{-2} d^{-1} were interpreted as due to local episodes of landslides inside the crater (and therefore were not volcanic fluctuations sensu stricto). Here, we arbitrarily chose a threshold equal to about 2 times the average, i.e., 5 kg m^{-2} d^{-1}. Obviously, any future peak in CO_2 flux requires a validation from the scientists involved in monitoring to rule out possible local effects, such as the above mentioned landslides.

[53] The threshold used for the strain rate is $\dot{\varepsilon} > 0$, because Mount Vesuvius has never experienced an inflation in the period of time it has been monitored (F. Pingue, personal communication, 2004). Finally, the threshold for the temperature of the fumaroles is chosen about 10% higher than the values observed since 1990 [*Chiodini et al.*, 2001].

[54] Now that we have defined unrest in terms of monitoring indicators, we can start to assign a probability to the node. We have no theoretical knowledge of the probability of unrest; therefore $p_a(\theta_1)$ is a uniform distribution. Past data are available to modify $p_a(\theta_1)$ into $p_b(\theta_1)$ through equation (5). In particular, we know that in the 384 months (32 years) of seismic observation, no unrest occurred, so $\alpha_b = 1$ and $\beta_b = 385$ in equation (6). Actually, only seismicity has been continuously monitored over this time

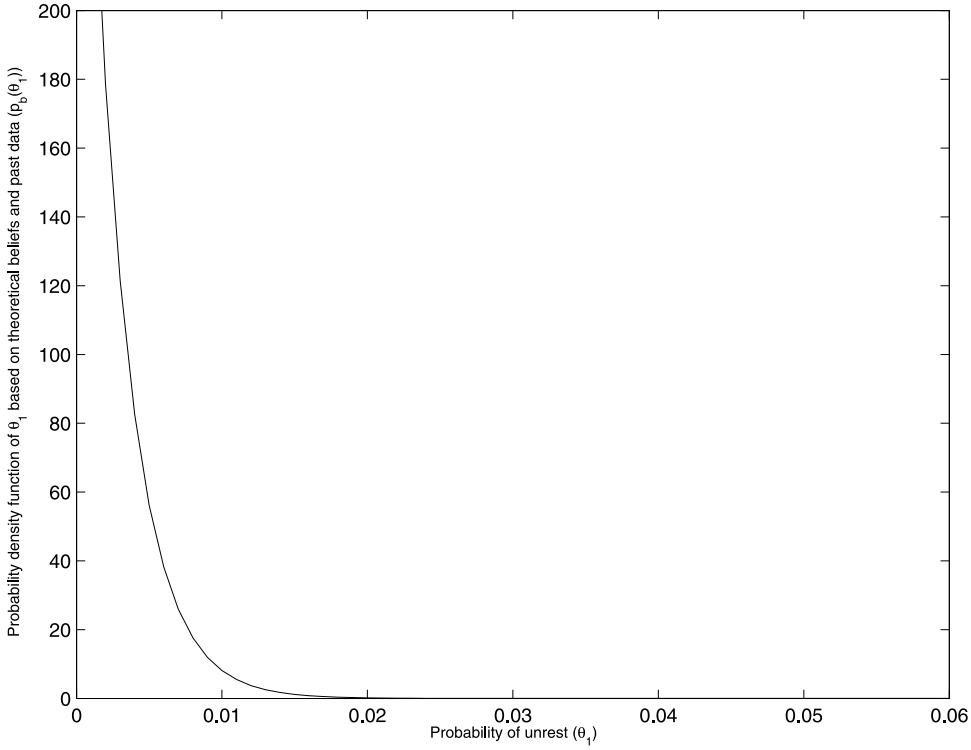

Figure 4. PDF of the probability of unrest based on a priori beliefs and past data ($p_b(\theta_1)$). The PDF is given by equations (6) and (A4), with $\alpha_b = 1$ and $\beta_b = 385$.

window, while measurements of ground deformation, temperature of the fumaroles, and gas emissions were carried out only in systematic surveys. We deduce that no unrest occurred in the last 32 years, because neither continuous nor periodic measurements, as well as no visual report from the people living in the surrounding of the volcano, have shown evidence of possible anomalies in this time interval. The variable $p_b(\theta_1)$ is plotted in Figure 4. Note that this procedure will probably overestimate the probability of occurrence of unrest because we neglect the time period between 1944 (last eruption) and 1971 owing to incomplete monitoring of the volcano, even though no unrest is known to have occurred.

[55] In this node the monitoring data modify $p_b(\theta_1)$ into $p_c(\theta_1)$ in a trivial way as previously mentioned. If unrest is observed (i.e., $Z_1 > 0$) we have $p_c(\theta_1) = \delta(\theta_1 - 1)$. On the other hand, if the monitoring data do not indicate the presence of unrest, the probability remains $p_b(\theta_1)$ that allows estimating the long-term hazard. Since we consider 32 years of data, the long-term hazard cannot be extrapolated beyond the next decade or so.

3.2.2. Node 2 (Origin): $p(\theta_2)$

[56] The theoretical information that can be used to assign a probability at this node are practically nonexistent. Unrest can be due to different factors, tectonic, magmatic, hydrothermal, etc., and it is impossible to anticipate the origin of unrest a priori on theoretical grounds. Furthermore, because no unrest has occurred since 1972 (at least), we assume conservatively that $p_b(\theta_2)$ has the form of a uniform distribution.

[57] In this node, monitoring data are used during unrest to modify the probability from $p_b(\theta_2)$ to $p_c(\theta_2)$. Unrest that definitely involves magma may eventually show some clear manifestation by erupting or by dike intrusion very close to the surface, but it is very hard to rule out the involvement of magma when there is unrest. The monitoring measurements for this node are selected on the basis of the considerations reported by NH02 looking at different volcanoes. According to NH02, those indicative of a magmatic origin for the unrest are Π_{SO_2}, the presence of significant SO_2 (0, no; 1, yes); $\dot{\varepsilon}$, the strain rate; $\overline{\nu}$, the dominant spectral frequency of earthquakes; ξ_e, the ratio between average and dispersion of the depth of the earthquakes during unrest; and T, the temperature of the fumaroles inside the crater. Formally speaking, equation (7) can be written as

$$Z_2 = 2z_{\Pi_{SO_2}} + z_{\dot{\varepsilon}} + z_{\overline{\nu}} + z_{\xi_e} + 2z_T \tag{11}$$

Here the weight is not the same for all the parameters. In particular, the presence of a significant amount of SO_2 and high temperature of the fumaroles inside the crater are considered strongly indicative of the presence of magma, so we have arbitrarily doubled their weights.

[58] These parameters and their thresholds are reported in Table 2. The threshold for T remains the same for the unrest (see Table 1). The threshold for $\dot{\varepsilon}$ is chosen by considering

Table 2. Node 2: Monitoring Parameters and Their Threshold

Parameter	Threshold
$z_{\Pi_{SO_2}} = 1$	$\Pi_{SO_2} = 1$
$z_{\dot{\varepsilon}} = 1$	$\dot{\varepsilon} \geq 10^{-5}$ d^{-1}
$z_{\overline{\nu}} = 1$	$\overline{\nu} \leq 3$ Hz
$z_{\xi_e} = 1$	$\xi_e < 0.40$
$z_T = 1$	$T > 105$°C

that a rapid and localized (usually positive) strain of the volcanic edifice is usually indicative of rising magma. The threshold in the dominant frequency of the earthquake spectrum is chosen according to *Chouet* [1996], and *McNutt* [2000]. For ξ_e, we use $\xi_e < 0.40$, which is about the ratio between the average and the dispersion of the depth of the earthquakes at Mount Vesuvius recorded in the last 30 years [cf. *Zollo et al.*, 2002]. We assume that earthquakes coming closer to the surface and/or occurring in a larger range of depths may indicate an upward migration of magma or a coalescence of small fractures that may facilitate the magma uprising. At the same time, we do not consider shallow earthquakes concentrated in a very small range of depth to be indicative of magma, as they could also be due to hydrothermal activity.

[59] As mentioned before, all of these parameters modify $p_b(\theta_2)$ into $p_c(\theta_2)$ during unrest. In particular, the average of $p_c(\theta_2)$ becomes

$$E_c[\theta_2] = \begin{cases} \frac{E_b[\theta_2]}{2} & \text{if} \quad Z_2 = 0 \qquad \text{(no APV)} \\ 1 - \exp^{-Z_2} & \text{if} \quad Z_2 \geq 1 \qquad \text{(at least 1 APV)} \end{cases} \tag{12}$$

[60] This shows a probability of magmatic origin increasing exponentially as the number of APVs of Z_2 increases. However, when all the measurements indicate 0, our interpretation is that the probability of a magmatic origin has to be decreased. It is difficult to admit a magmatic origin when none of these measurements shows it, although not impossible. For this reason, $E_c[\theta_2]$ is arbitrarily set to $E_b[\theta_2]/2$. The variance is set through equation (A6) in Appendix A by using the new average $E_c[\theta_2]$.

3.2.3. Node 3 (Outcome): $p(\theta_3)$

[61] We start from an almost total ignorance about preeruptive processes when Mount Vesuvius is in a closed vent condition, so we assume that $p_a(\theta_3)$ is a uniform distribution. No pertinent historical data exist. Therefore $p_b(\theta_3)$ remains an uniform distribution.

[62] Monitoring data can modify $p_b(\theta_3)$ into $p_c(\theta_3)$ once unrest occurs. The monitoring measurements, indicative of magma rising to the surface, have been selected on the basis of NH02 and references therein, *Voight and Cornelius* [1991], *Chouet* [1996], *Kilburn* [2003], and *Sparks* [2003]. Some parameters and the relative thresholds have been selected by simple subjective inferences from real recent eruptions such as Pinatubo [see *Newhall and Punongbayan*, 1996], Mount St. Helens [*Lipman and Mullineaux*, 1981], and Montserrat. The most important point is that we are assuming that the parameters listed below represent an almost complete set of possible scenarios of phenomena occurring before an explosive eruption in a volcano characterized by a "closed" conduit regime. In particular, we consider the following parameters:

- PE presence of phreatic explosion (0, no; 1, yes);
- $\dot{\bar{\nu}}$ rate of change of the average spectral frequency content of earthquakes;
- ξ_e ratio between average and dispersion of the depth of the earthquakes during unrest;
- $\ddot{E}$ acceleration of seismic energy release;
- $\ddot{\varepsilon}$ acceleration of inflation;
- ε cumulative strain since the beginning of the unrest;
- $\dot{\rho}$ change of the ratios HCl/SO_2 and/or HF/SO_2;
- REV sudden reversal of at least one of the above parameters (0, no; 1, yes).

Table 3. Node 3: Monitoring Parameters, Thresholds, and Their Typical Lead Times Observed Before Eruptions

Parameter	Threshold	Lead Time
$z_{PE} = 1$	PE = 1	days to months
$z_{\dot{\bar{\nu}}} = 1$	$\dot{\bar{\nu}} < 0$	hours to few weeks
$z_{\xi_e} = 1$	$\xi_e < 0.40$	hours to few weeks
$z_{\ddot{E}} = 1$	$\ddot{E} > 0$	hours to few days
$z_{\ddot{\varepsilon}} = 1$	$\ddot{\varepsilon} > 0$ d^{-2}	hours to few days
$z_{\varepsilon} = 1$	$\varepsilon > 10^{-4}$	hours to weeks
$z_{\dot{\rho}} = 1$	$\dot{\rho} > 0$	few days
$z_{REV} = 1$	REV = 1	hours to few days

[63] Formally speaking, equation (7) is written as

$$Z_3 = 2z_{PE} + z_{\dot{\bar{\nu}}} + z_{\xi_e} + z_{\ddot{E}} + 2z_{\ddot{\varepsilon}} + z_{\varepsilon} + z_{\dot{\rho}} + 2z_{REV} \tag{13}$$

The weight is not the same for all of the parameters. In particular, we assign a double weight ($\omega = 2$) to the observation of phreatic explosions (PE), to the observation of an acceleration of uplift ($\ddot{\varepsilon}$), and to a sudden reversals of some measured parameters (REV) because they are strong indicators that magma is reaching the surface.

[64] The parameters, thresholds, and lead times (see below) are reported in Table 3. The threshold of ε (10^{-4}) represents a reasonable value for the maximum prefracture strain [e.g., *Kanamori*, 1980]. For the other parameters the thresholds are based on a "yes/no" choices. In most cases, in fact, the threshold is set to 0 because they are derivatives of monitored variables and we are interested in the time trend of their primitive functions. For PE and REV we do not need any threshold value since it is sufficient to observe them, regardless of how intense they are.

[65] As mentioned before, monitored unrest modifies $p_b(\theta_3)$ into $p_c(\theta_3)$. In particular, the probability average of $p_c(\theta_3)$ becomes

$$E_c[\theta_3] = \begin{cases} \frac{E_b[\theta_3]}{5} & \text{if} \quad Z_3 = 0 \qquad \text{(no APV)} \\ 1 - \exp^{-Z_3} & \text{if} \quad Z_3 \geq 1 \qquad \text{(at least 1 APV)} \end{cases} \tag{14}$$

[66] As for node 2, when the z_i values for all measured variables are 0, our interpretation is that the probability of occurrence of an eruption has to be decreased. In such a case, $E_c[\theta_3]$ is arbitrarily set to $E_b[\theta_3]/5$ because it is unlikely that an eruption will occur if there are no APVs in this node. Also in this case, the variance is set through equation (A6) in Appendix A by using the new mean $E_c[\theta_3]$.

[67] A very important feature of this node (as well as for node 1) is that the probability is expressed in terms of a time interval τ. In fact, when we observe data that indicate that magma is reaching the surface, we also have to specify "when", most likely, this will happen. Here, we set τ = 1 month (see above), but this choice has to be carefully discussed. Z_3 is obtained by eight parameters. Each of them is characterized by a different lead time, i.e., the time lag between the observation of an APV in node 3 and the most likely occurrence of the impending eruption. In Table 3 we report typical lead times, which can range from few hours to

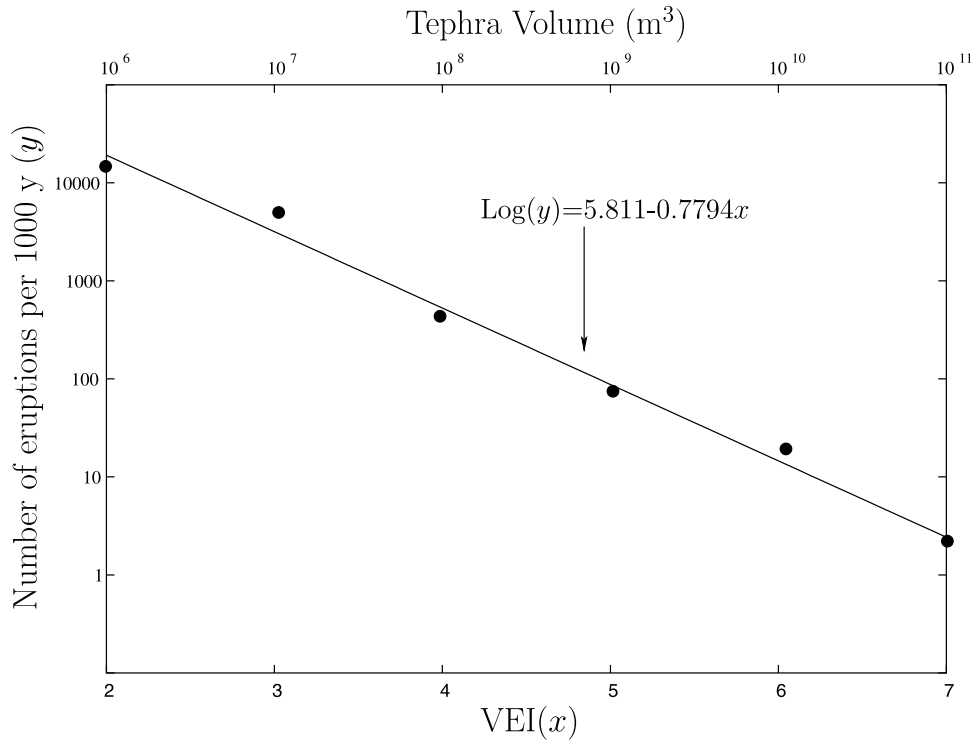

Figure 5. VEI versus frequency of Holocene eruptions, worldwide [from *Simkin and Siebert*, 1994]. The line is the best fitting line determined using the data points shown. The equation is given.

months. Our choice to set τ = 1 month represents a very rough average value, overall.

[68] The large uncertainty in the lead times is very awkward. A reliable estimation of the lead time would be very useful to design efficient risk reduction, for instance, moving the people from danger areas. At the present state of knowledge, we think the reduction of this large uncertainty can be obtained only in some specific case where the precursors have some kind of "regular" behavior like few days before the Pinatubo eruption in 1991. We think, however, we should consider such a "regular" behavior as an exception rather than a rule. More likely, if we want to have enough time to move people from danger areas around Mount Vesuvius, we will not be able to wait for unequivocal signals that usually occur just a few hours to few days before eruptions. Recognizing this, the authorities have recently promoted a long-term plan to encourage people to more from their homes in the surroundings of Mount Vesuvius and to go to live in safer areas. If this long-term plan will have success, potentially it can lead to a reduction of the time interval needed to evacuate the surroundings of Mount Vesuvius before a possible impending eruption.

[69] In summary, our choice to set τ = 1 month must not be taken as an indication that we are able to make a reliable forecast of an impending eruption 1 month beforehand. Table 3 shows that the more reliable lead times can be very short, much less than 1 month. That said, we should also be ready to face the possibility that an eruption might only occur several months after the alarm level has been reached.

[70] At this stage, other probabilities may be relevant for practical purposes. The product of the probabilities of the first three nodes gives the probability of eruption in a time interval τ. The complementary value, i.e.,

$$P^{\star} = 1 - p(\theta_1)p(\theta_2)p(\theta_3) \tag{15}$$

is the probability to have no eruption. During unrest, P becomes

$$P^{\star} = 1 - p(\theta_2)p(\theta_3) \tag{16}$$

and it could be interpreted also as the probability to have a "failed unrest." Here, we intentionally avoid the term "false alarm" because we can evaluate the probability of a false alarm only when a "warning" is given.

3.2.4. Node 4 (Magnitude): $p(\theta_4^{(VEI)})$

[71] This node is maybe the most critical from a practical point of view because it allows testing the MEE hypothesis.

3.2.4.1. A Priori Model ($p_a(\theta_4^{(VEI)})$)

[72] The explosive magnitude of an eruption is characterized most simply by the Volcanic Explosivity Index (VEI) [*Newhall and Self*, 1982]. For complex natural systems, the frequency-magnitude (i.e., the VEI) relationship generally follows a power law, as in the Gutenberg-Richter law for earthquakes [e.g., *Bak and Tang*, 1989; *Woo*, 1999]. This propensity is informative: in Figure 5 we depict the power law estimated by considering all the historically known volcanic eruptions [*Simkin and Siebert*, 1994], with VEI $\geq$ 2. Since Mount Vesuvius is presently in a closed conduit regime, with little degassing [cf. *Frondini et al.*, 2004], we argue that the next event has to have a minimum energy to reopen the conduit. For this reason, we assume the likelihood is negligible that the next eruption at Mount

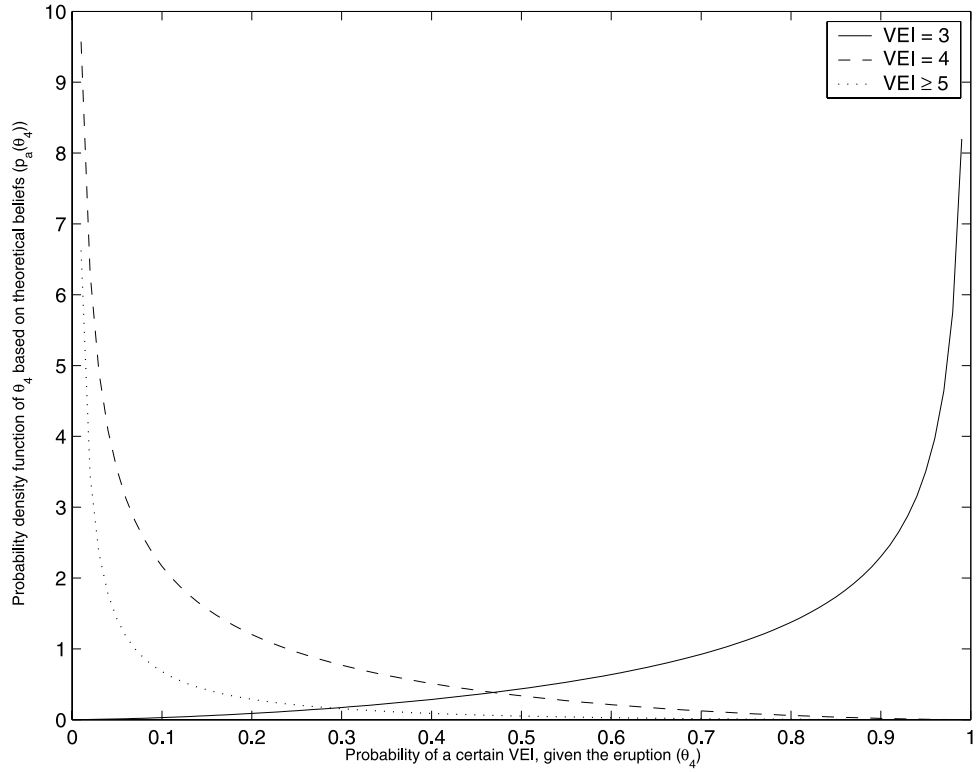

Figure 6. Marginal PDFs of the probability of a specific VEI given that there is an eruption, based on a priori beliefs ($p_a(\theta_4^{(VEI)})$); solid line for VEI = 3, dashed for VEI = 4, and dotted for VEI $\geq$ 5 eruption. The PDFs are given by equations (A1) and (A4) using the parameters in Table 4 (see Appendix A for more details).

Vesuvius will have a VEI of 2 or smaller. In other words, we assume that the power law of Figure 5 reflects our a priori theoretical knowledge for this node but with a minimum possible VEI = 3.

[73] In this case, the marginal distribution of each specific VEI is a Beta distribution centered around a value given by the power law distribution [see, e.g., *Aki*, 1965]. At this stage the variance is the maximum allowed for the average considered. In Figure 6, we report the distributions for VEI $\geq$ 5 ($p_a(\theta_4^{(5+)})$), VEI = 4 ($p_a(\theta_4^{(4)})$) and VEI = 3 ($p_a(\theta_4^{(3)})$), while in Table 4 we report the values used for the parameters of the marginal Beta distribution.

3.2.4.2. Past Data ($p_b(\theta_4^{(VEI)})$)

[74] Also in this case, past data can be used to improve the probability estimation, i.e., modifying $p_a(\theta_4^{(VEI)})$ into $p_b(\theta_4^{(VEI)})$. We use three different types of data: (1) the worldwide eruption catalog; (2) the eruption catalogs of the volcanoes with behavior and products similar to Mount Vesuvius (so-called "analogs"); and (3) the eruption catalog of Mount Vesuvius. The VEI of each Mount Vesuvius eruption is estimated from the tephra volume and the column height given by *Cioni et al.* [2003]. The magnitude-frequency relation and chronology for all volcanoes is from *Simkin and Siebert* [1994]. To select analogs, we use two main criteria: (1) a pronounced alternation between open and closed conduit behavior in the volcano's geological or historical record and (2) the viscosity of magma contained in a range that includes all but the most acid (e.g., rhyolites) [see *Romano et al.*, 2003]. We have identified seventeen volcanoes (Suwanose-jima, Sakura-Jima, Popocatepetl, Shikotsu-Tarumai, Fuji, Alaid, Shiveluch, Trident, Komaga-Take, Asama, Colima, Fuego, Mayon, Arenal, Cotopaxi, Tungurahua, Merapi) that best match the above criteria.

[75] The main scientific question concerns the role of the repose time. We know that Mount Vesuvius has been quiescent for the last 60 years. How does this information affect our estimate of $p_b(\theta_4^{(VEI)})$? The Poisson hypothesis used in some previous papers assumes that the repose time is not relevant to estimate the probability of occurrence, timing, and the size of the next eruption [see, i.e., *Scandone et al.*, 1993a; *Lirer et al.*, 2001]. On the other hand, it has been observed from volcanoes worldwide [e.g., *Simkin and Siebert*, 1994; NH02; *Sandri et al.*, 2003] that large explosive eruptions are often associated with long repose times. Geological and historical records seem to confirm the same behavior also for Mount Vesuvius [*Santacroce*, 1983].

Table 4. Node 4: Values of the Parameters of the Dirichlet Distribution for $p_a(\theta_4)$[a]

VEI	Parameters Dirichlet Distribution
3	$\alpha_{a1} = 2.49$
4	$\alpha_{a2} = 0.42$
$\geq$5	$\alpha_{a3} = 0.09$

[a]The parameters are obtained by imposing the averages of the Beta marginal distributions (see equation (A2)) equal to the values given by the power law distribution of Figure 5 (see text for more details).

Table 5. Node 4: Expected Values of the Distributions of $p_b(\theta_4^{(VEI)})$ for Different Choices of Data Set of Past Measurements[a]

Class	$E_b[\theta_4^{(VEI=3)}]$	$E_b[\theta_4^{(VEI=4)}]$	$E_b[\theta_4^{(VEI\geq 5)}]$
A4	0.68	0.30	0.02
B4	0.63	0.23	0.14
C4	0.72	0.27	0.01
D4	0.60	0.30	0.10
E4	0.57	0.23	0.20
F4	0.65	0.24	0.11

[a]See Figure 7.

[76] However, are long repose times always followed by large VEI eruptions? The relationship between repose time (RT) and VEI is very complex. We think a correct interpretation of such a link has to take also into account the effect of other parameters. In particular, we argue that degassing during repose may play a major role. From a mechanical point of view, a long RT favors the closure of the conduit due to the viscoelasticity and the cooling of the rocks of the conduit [i.e., *Quareni and Mulargia*, 1993]. Overall, this behavior tends to facilitate the recharging of the system, by increasing the resistance of the volcano to bear overpressure in the magma chamber. On the other hand, the presence of a large fracture or convection system can play an important role in this process, favoring a significant level of degassing. A strongly degassed magma is apparently less capable of large VEIs [*Newhall et al.*, 1994; *Newhall*, 2003]. Therefore strong degassing may allow very long RTs and yet still produce small VEI eruptions.

[77] We envision two limiting cases that define a wide range of possible models, and that probably encompass the most realistic model: in one case, a long RT allows the system to switch into a "closed conduit regime." If the magnitudes of eruptions are mainly controlled by complex geophysical, geochemical and geomechanical factors in the reopening of the conduit, they will exhibit a power law distribution in terms of size (as for any complex system [see *Bak et al.*, 1988]). In the other case, if we assume a stationary recharging of the system, and very simple physical mechanisms in reopening the conduit, we might expect, on average, to see some kind of linear relationship between VEI and RTs.

[78] As we are presently unable to discriminate between these limiting cases, we therefore estimate $p_b(\theta_4^{(VEI)})$ by considering two different families of classes: in one family (A4, B4, and C4), we select the past eruptions with a RT longer than 60 years and shorter than 200 years; in the other family (D4, E4, and F4), we take all the past eruptions with a RT longer than 60 years. The first family assumes that there is a significant difference in the RTs of VEI = 4 and larger eruptions. Under this assumption, since Mount Vesuvius has been quiescent for "only" 60 years, it would not be appropriate to include eruptions with very long RTs (e.g., several centuries or more). On the other hand, the other family is based on the assumption that RTs of few decades or several centuries "influence" in a similar way the magnitude of the next eruption (see conceptual model described above). Hence data on any RTs that are longer than 60 years is informative.

[79] In Tables 5 and 6 and Figure 7 we report $p_b(\theta_4^{(VEI)})$ for these different classes. More specifically, for the first family we derive the A4 class by considering the past frequency of different VEIs in a worldwide catalog. In this context, *Simkin and Siebert* [1994] display a table with such frequencies grouped for RT in powers of 10. Because of this, in the A4 class we consider the worldwide occurrence of volcanic eruptions with a repose time between 10 and 100 years. Relative to the same family of classes, the B4 class is based on the available analogs, selecting all those eruptions which occurred at these volcanoes with a RT between 60 and 200 years. The last class for the same family (C4 class) involves considering the Mount Vesuvius historical eruptions with a RT between 60 and 200 years [*Cioni et al.*, 2003; *Simkin and Siebert*, 1994]. In the second family of classes (D4, E4, and F4), we use the same data sets as above, but consider the eruptions with a RT longer than 60 years, without an upper limit.

[80] The most relevant insight is that the probability that the next eruption will be larger than MEE (i.e., VEI $\geq$ 5) is not less than 1% (see Table 5), and ranges from 1 to 20%. It is also worth noting that the result of the class with the lowest probability (i.e., C4: Mount Vesuvius data with 60 $\leq$ RT $\leq$ 200 years) is strongly influenced by the fact that the only VEI $\geq$ 5 in the catalog (the 79 A.D. Pompeii eruption) has a RT of about 300 years, which is longer by a factor of 2 than the RT of the VEI = 4 eruptions.

[81] In order to properly account for the uncertainties attached to each probability estimation reported in Table 5, we also evaluate for each class the likelihood that the real (unknown) probability of VEI $\geq$ 5 events are >1%, and therefore (by our definition) "not negligible." In Table 7 we report the results for the different classes. Note that the probabilities are almost all very high and, in every case, higher than 10%. In practice, this means that the probability

Table 6. Node 4: Different Choices of Data Set of Past Measurements Used to Estimate $p_b(\theta_4)$

	A4 Class	B4 Class	C4 Class	D4 Class	E4 Class	F4 Class
Eruptions	worldwide	analogs	Mount Vesuvius	worldwide	analogs	Mount Vesuvius
RT, years	$10 \leq RT < 100$	$60 \leq RT < 200$	$60 \leq RT < 200$	≥ 10	≥ 60	≥ 60
N	307	12	6	581	17	7
VEI = 3						
n	208	7	4	347	9	4
α_{b1}	210.5	9.5	6.5	349.5	11.5	6.5
VEI = 4						
n	92	3	2	173	4	2
α_{b2}	92.4	3.4	2.4	173.4	4.4	2.4
VEI $\geq$ 5						
n	7	2	0	61	4	1
α_{b3}	7.1	2.1	0.1	61.1	4.1	1.1

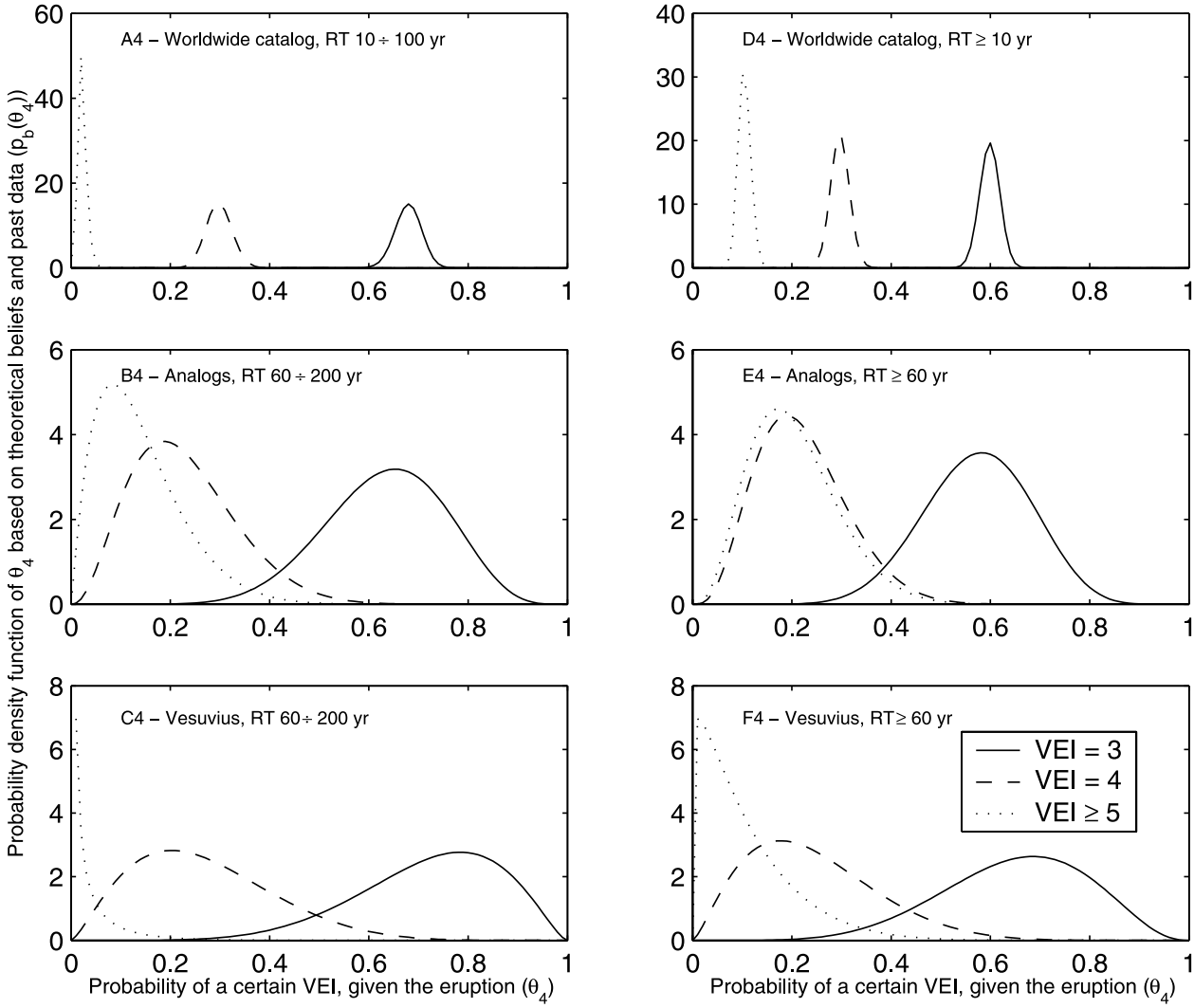

Figure 7. PDF of the probability of a specific VEI given that there is an eruption, based on a priori beliefs and past data ($p_b(\theta_4^{(VEI)})$) for different classes: (left) (top) class A4, (middle) class B4, and (bottom) class C4. (right) Results for classes D4, E4, and F4. In each plot, curves for different values of VEI are shown: solid line for VEI = 3, dashed line for VEI = 4, and dotted line for VEI $\geq$ 5 eruption.

of occurrence of a VEI $\geq$ 5 eruption cannot be considered negligible in all classes used.

[82] This outcome differs from what is presently assumed by the Emergency Plan of Mount Vesuvius. As mentioned before, the existing plan assigns a maximal VEI = 4 to the MEE for the next eruption [cf. *Cioni et al.*, 2003]. In contrast, our model assesses a probability for each possible VEI, and finds a nonnegligible probability of a VEI $\geq$ 5 event. From a physical point of view, eruptive mechanisms have so much intrinsic aleatoric uncertainty (as with all complex systems), and/or our knowledge is too rudimentary to make precise and unequivocal (i.e., "deterministic") prediction of the magnitude of the next event.

3.2.4.3. Monitoring Data ($p_c(\theta_4^{(VEI)})$)

[83] With our present state of knowledge, monitoring data does not seem able to provide help in estimating the VEI of an impending eruption [*Sandri et al.*, 2003], in large part due to random factors (as for any complex system). This issue, however, is still worthy of study: as mentioned before, for instance, degassing during repose may play a major role in limiting the magnitude of a subsequent eruption. In this regard, important measurements are gas emission data, and the computation of gas balances in the volcanic system [*Newhall et al.*, 1994; *Newhall*, 2003]. Also monitoring data can help to assess the plausibility of lateral blasts: for example, the lateral blast at Mount St. Helens was preceded by a strong and localized deformation on a flank of the volcano that produced a gravitational instability. At

Table 7. Probability That the Real (Unknown) Probability of a VEI $\geq$ 5 Event Is >1%

Class	Probability
A4	0.97
B4	>0.99
C4	0.17
D4	>0.99
E4	>0.99
F4	0.93

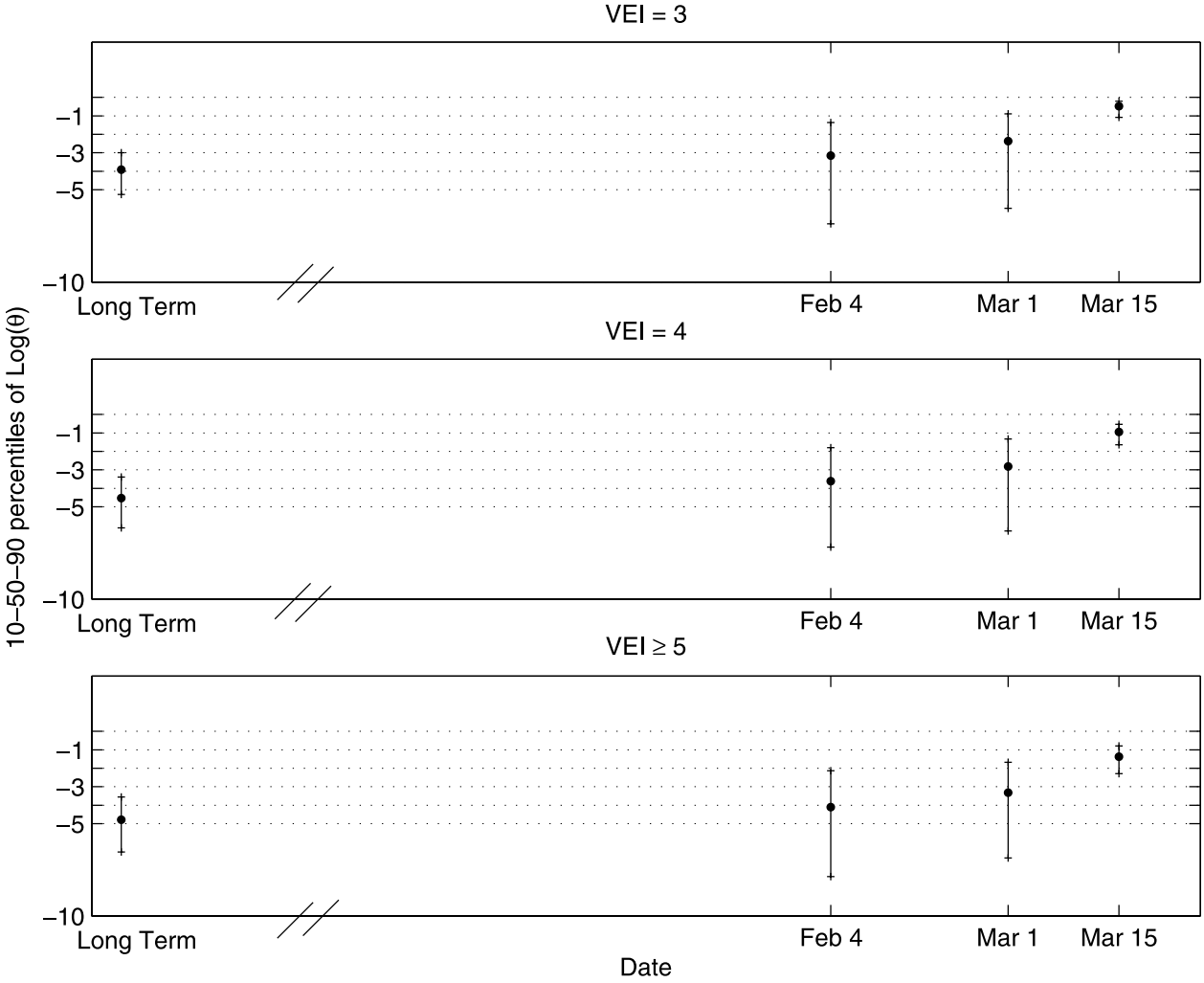

Figure 8. Time evolution of the 10, 50, and 90 percentiles of the probability of eruption per month for the hypothetical unrest crisis described in section 4 for the F4 class. Probabilities (top) for a VEI = 3 eruption, (middle) for a VEI = 4 eruption, and (bottom) for a VEI $\geq$ 5 eruption. Note the log scale on the y axis.

this stage, however, monitoring data are not included into the calculation of probability at this node for the Mount Vesuvius case.

4. Calculating the Hazard: A Hypothetical Example

[84] In order to illustrate the hazard assessment at Mount Vesuvius we provide a hypothetical example consisting of the time evolution of a possible future preeruptive scenario. We calculate the hazard at different (fictitious) times: (1) 3 February, no unrest observed, (2) 4 February, slight inflation of the volcano ($\dot{\varepsilon} \simeq 5 \times 10^{-6}\,\mathrm{d}^{-1}$), (3) 1 March, the slight inflation continues; occurrence of LF events at a mean depth of 2.5 km, with an average spectral frequency of 3 Hz, and (4) 15 March, the same as 1 March, but the mean depth of hypocenters of the LF events is now at 1 km depth and the average spectral frequency is decreased to 1–2 Hz.

[85] In Figure 8, we report the time evolution of the probability distribution (10, 50 and 90 percentiles) for a VEI = 3, VEI = 4 (the MEE), and VEI $\geq$ 5 eruption at different times by using the F4 class. The probability of a specific VEI is defined as a combination of the probabilities at each node [e.g., *Gelman et al.*, 1995]. For instance, the probability to have a VEI = 3 eruption in the next N_τ months when unrest is not occurring is

$$p(\mathrm{VEI}=3) = p_b(\theta_1)p_b(\theta_2)p_b(\theta_3)p_b\left(\theta_4^{(3)}\right)N_\tau \qquad (17)$$

When unrest is occurring, the probability to have a VEI = 3 eruption in the next month is

$$p(\mathrm{VEI}=3) = p_c(\theta_2)p_c(\theta_3)p_b\left(\theta_4^{(3)}\right) \qquad (18)$$

[86] In practice, we first simulate 1000 random outcomes from the probability distribution of each node. Then, we multiply each single random output with other single outputs of the other nodes. Therefore we obtain 1000 random values that represent a random sampling from p(VEI = 3).

[87] Figure 8 gives the probability of eruptions at different times for different VEIs. Before "3 February" (the quiet

period) the average of the probability for a VEI ≥ 4 eruption is about 3×10^{-4} month^{-1} (the probability interval defined by the 10th and 90th percentiles is 0.4×10^{-5} to 0.6×10^{-3} month^{-1}). This value is similar to the estimate 2×10^{-3} yr^{-1} given by *Scandone et al.* [1993a]. Similar steps yield revised estimates of mid- to short-term probabilities on 4 February, 1 March, and 15 March, which illustrate the way the hazard changes with time.

5. Final Remarks

[88] The main purpose of this paper is to outline a new approach to estimate the probability of eruption based on a statistical implementation of the event tree scheme [*Newhall and Hoblitt*, 2002]. We then applied the technique to estimate the current level of volcanic hazard at Mount Vesuvius. The approach emphasizes a practical application, merging all the available information, a priori beliefs and models, past data, and monitoring observations.

[89] The method allows the estimation of the long-term hazard during a quiet period (useful for land use policy), and is perhaps most useful for estimating in "real time" the mid- to short-term probability of eruption depending on any monitoring data observed during unrest. The assessment provides also an estimate of the probability of "failed unrest" that may be very useful for people who manage volcanic crises.

[90] From a scientific point of view, the method has many interesting properties. For instance, it recognizes and deals with the aleatoric (intrinsic) and epistemic (due to the scarce knowledge) uncertainties in a formally correct way. Besides these formal aspects, the results are very important for comparing appropriately exposure due to different hazards, and may guide future research whose aim is to reduce epistemic uncertainties.

[91] Finally, the method provides a means for merging together all the available information (theoretical, historical, geological, and monitoring) that is pertinent to a scientific assessment of hazard. The rules adopted here to define the probabilistic event tree for Mount Vesuvius can be applied to similar volcanoes. However, individual thresholds would need to be modified in accordance with the background activity of the volcano considered.

Appendix A

[92] In our Bayesian model we assume θ_k is a random variable with a Dirichlet distribution

$$p(\theta_k) = \frac{\Gamma(\alpha_1 + \ldots + \alpha_m)}{\Gamma(\alpha_1)\ldots\Gamma(\alpha_m)} \left[\theta_k^{(1)}\right]^{\alpha_1 - 1} \ldots \left[\theta_k^{(m)}\right]^{\alpha_m - 1} \quad \text{(A1)}$$

where $\alpha_j > 0$, $\theta_k^{(1)}, \ldots, \theta_k^{(m)} > 0$, $\sum_{j=1}^{m} \theta_k^{(j)} = 1$, and m is the number of possible mutually exclusive and exhaustive events.

[93] The first two moments of the distribution are

$$E\left[\theta_k^{(j)}\right] = \frac{\alpha_j}{\alpha_0} \quad \text{(A2)}$$

$$\mathrm{Var}\left[\theta_k^{(j)}\right] = \frac{\alpha_j(\alpha_0 - \alpha_j)}{\alpha_0^2(\alpha_0 + 1)} \quad \text{(A3)}$$

where $\alpha_0 \equiv \sum_{j=1}^{k} \alpha_j$.

[94] In the case $m = 2$ (e.g., magma or not) and for events not mutually exclusive, the Dirichlet distribution becomes a Beta distribution

$$p(\theta_k) = \mathrm{Beta}(\alpha, \beta) = \frac{\Gamma(\alpha + \beta)}{\Gamma(\alpha)\Gamma(\beta)} \theta_k^{\alpha - 1}(1 - \theta_k)^{\beta - 1} \quad \text{(A4)}$$

where $\alpha, \beta > 0$, and a sufficient condition to have a finite PDF is $\alpha, \beta \geq 1$ [e.g., *Gelman et al.*, 1995]. Very often (but not necessarily), α and β are integers related to the number of available data; in this case, $\alpha - 1$ is the number of successes, and $\beta - 1$ the number of failures. Remarkably, also the marginal distribution of a specific $\theta_k^{(j)}$ in the more general case ($m > 2$) is Beta(α_j, $\alpha_0 - \alpha_j$).

[95] The first two moments of the Beta distribution, $E[\theta_k]$ (the mean) and $E[\theta_k^2]$ (the variance), are

$$E[\theta_k] = \frac{\alpha}{\alpha + \beta} \quad \text{(A5)}$$

$$E\left[\theta_k^2\right] = \mathrm{Var}[\theta_k] = \frac{\alpha\beta}{(\alpha + \beta)^2(\alpha + \beta + 1)} = E[\theta_k](1 - E[\theta_k])\frac{1}{\alpha + \beta + 1} \quad \text{(A6)}$$

[96] In general, the average of the Beta distribution represents an estimation of the aleatoric uncertainty, i.e., the intrinsic (and unavoidable) random variability due to the complexity of the process. The dispersion around the central value (i.e., the variance), instead, represents an estimation of the epistemic uncertainty, due to our limited knowledge of the process. In spite of the latter being neglected in past works, its estimation is very important for correct comparison between the probabilities of different hazards, and the confidence limits that are ascribed to them [cf. *Gelman et al.*, 1995; *Woo*, 1999].

[97] The Beta distribution has two important limiting cases. The case of $\alpha = \beta = 1$ represents the uniform distribution; in this case the mean and variance are

$$E[\theta_k] = \frac{1}{2} \quad \text{(A7)}$$

$$\mathrm{Var}[\theta_k] = \frac{1}{12} \quad \text{(A8)}$$

[98] On the other hand, when α (or β) $\rightarrow \infty$, Var $[\theta_k] \rightarrow 0$. This means that the Beta distribution tends to a Dirac's δ distribution centered around the average. In practice, this means then when we have a large amount of information the epistemic uncertainty becomes negligible.

[99] The concepts of aleatoric and epistemic uncertainties and their link to the Beta distribution can be described by discussing the Ellsberg paradox. In this case, we have two urns with 100 black and white balls (see Figure A1); we know that one urn contains 50 black balls and 50 white balls, while in the other we do not have any a priori information on the proportion of black and white balls. The probability of getting a black ball from a single drawing from the first urn can be described by a Dirac distribution

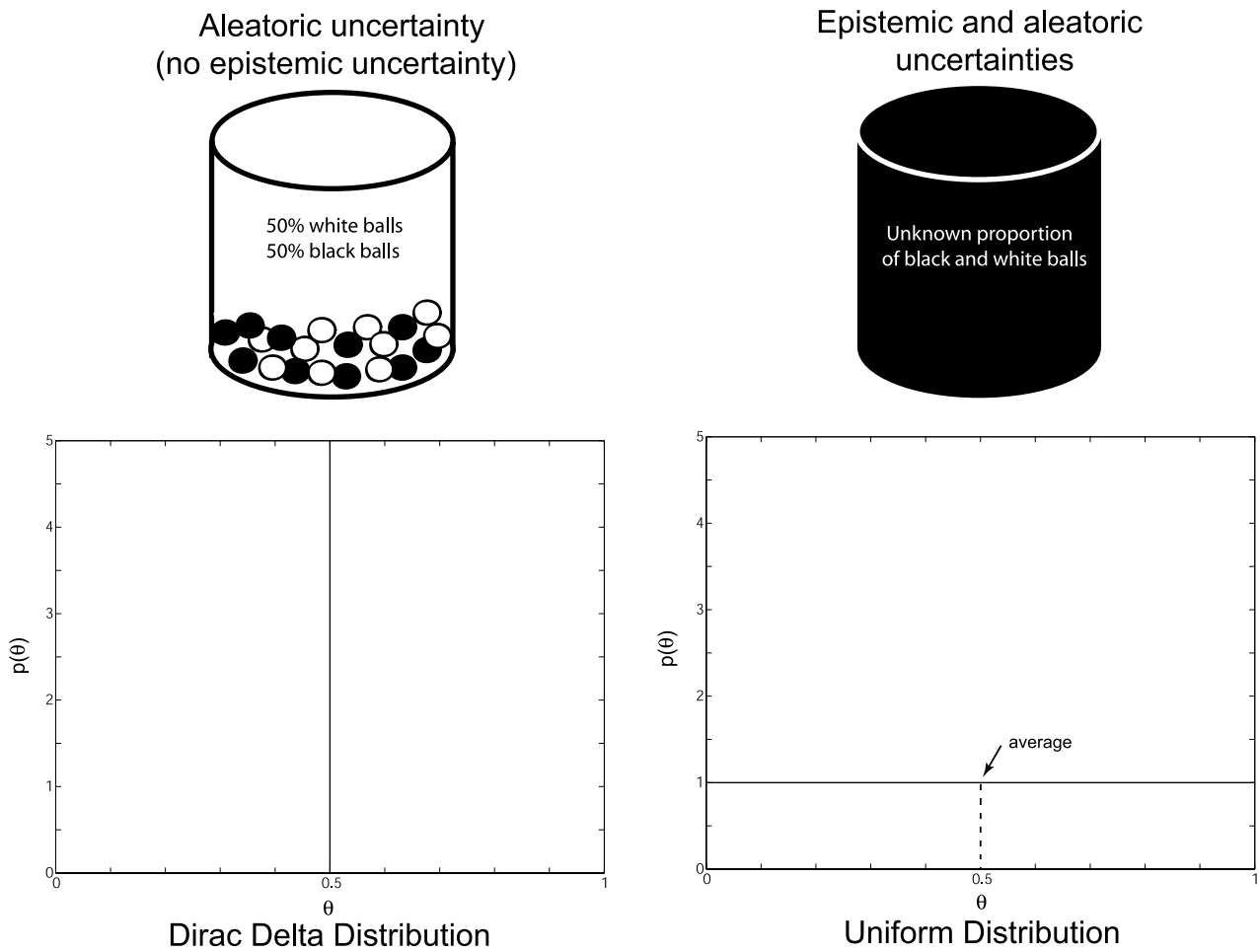

Figure A1. The Ellsberg paradox. (left) An urn with identical proportions of black and white balls and the Beta distribution (a Dirac distribution) that describes the system. (right) An urn with black and white balls in unknown proportions and the Beta distribution (the uniform distribution) that describes the system. In this case θ is the probability to obtain a black ball on a single trial, and $p(\theta)$ is its statistical distribution. See Appendix A for more details.

centered around 0.5, that is, the aleatoric uncertainty of the system; here the epistemic uncertainty is zero because we know the system perfectly. The probability of drawing a black ball from the second urn is described by a uniform distribution because the real proportion of black and white balls can be any value between 0 and 1; here the estimation of the aleatoric uncertainty is 0.5 (the average of the uniform distribution), while the epistemic uncertainty is the maximum allowed. For a single trial, the two urns are equivalent because the average is the same. However, in a long run of bets, we expect to eventually obtain the same number of white and black balls from the first urn, and the observations (i.e., the output of the drawings) do not modify our probability scheme. For the second urn, we have to add recursively (Bayesian logic) the outcome of each drawing into our probability model, in order the average of the Beta distribution to converge toward the real aleatoric uncertainty (the proportion of black and white balls).

[100] As final consideration, we are aware that the choice of the Beta distribution to represent probabilities is itself rather subjective, and in some case probabilities may be more appropriately characterized by other distributional forms. However, any possible bias introduced by this subjective choice is certainly less than assuming an exact value for the probability, that is, assuming a Dirac's δ distribution. Actually, the latter is a much more subjective choice because it neglects the epistemic uncertainty.

[101] **Acknowledgments.** This work has greatly benefitted from several discussions with many colleagues at the Osservatorio Vesuviano-INGV. A special thank to G. Macedonio, G. Chiodini, E. Del Pezzo, M. Martini, and F. Pingue, who gave us very useful monitoring information and interesting suggestions. We also thank Lee Siebert (Smithsonian Institution) for providing us data from worldwide volcanoes and Jim Kauahikaua, Dave Hill, and Willy Aspinall, who reviewed the manuscript improving significantly the readability of the paper. The work has been financially supported by GNV funds and by the European project e-Ruption.

References

Aki, K. (1965), Maximum likelihood estimate of *b* in the formula log(*N*) = *a* − *bM* and its confidence limits, *Bull. Earthquake Res. Inst. Univ. Tokyo*, *43*, 237–239.

Aspinall, W. P., and G. Woo (1994), An impartial decision-making procedure using expert judgment to assess volcanic hazards, in *Large Explosive Eruptions*, *Atti Conv. Lincei*, vol. 112, pp. 211–220, Accad. Naz. dei Lincei, Rome.

Aspinall, W. P., G. Woo, B. Voight, and P. J. Baxter (2003), Evidence-based volcanology: Application to eruption crises, *J. Volcanol. Geotherm. Res.*, *128*, 273–285.

Bak, P., and C. Tang (1989), Earthquakes as a self-organized critical phenomenon, *J. Geophys. Res.*, *94*, 15,635–15,637.

Bak, P., C. Tang, and K. Wiesenfeld (1988), Self-organized criticality, *Phys. Rev. A*, *38*, 364–374.

Barberi, F., G. Macedonio, M. T. Pareschi, and R. Santacroce (1990), Mapping the tephra fallout risk: An example from Vesuvius, Italy, *Nature*, *344*, 142–144.

Capuano, P., , P. Gasparini, A. Zollo, J. Virieux, R. Casale, and M. Yeroyanni (Eds.) (2003), *The Internal Structure of Mt. Vesuvius*, Off. Graf. Liguori, Naples, Italy.

Chiodini, G., L. Marini, and M. Russo (2001), Geochemical evidence for the existence of high-temperature hydrothermal brines at Vesuvio volcano, Italy, *Geochim. Cosmochim. Acta*, *65*, 2129–2147.

Chouet, B. A. (1996), Long-period volcano seismicity: Its source and use in eruption forecasting, *Nature*, *380*, 309–316.

Chouet, B. A., R. A. Page, C. D. Stephens, J. C. Lahr, and J. A. Power (1994), Precursor swarms of long-period events at Redoubt volcano (1989–1990), Alaska: Their origin and use as a forecasting tool, *J. Volcanol. Geotherm. Res.*, *62*, 95–135.

Cioni, R., A. Longo, G. Macedonio, R. Santacroce, A. Sbrana, R. Sulpizio, and D. Andronico (2003), Assessing pyroclastic fall hazard through field data and numerical simulations: Example from Vesuvius, *J. Geophys. Res.*, *108*(B2), 2063, doi:10.1029/2001JB000642.

Del Pezzo, E., F. Bianco, and G. Saccorotti (2003), Duration magnitude uncertainty due to seismic noise: Inferences on the temporal pattern of G-R b-value at Mount Vesuvius, *Bull. Seismol. Soc. Am.*, *93*, 1847–1853.

De Natale, G., S. M. Petrazzuoli, C. Troise, F. Pingue, and P. Capuano (2000), Internal stress field at Mt. Vesuvius: A model for background seismicity at a central volcano, *J. Geophys. Res.*, *105*, 16,207–16,214.

Esposti Ongaro, T., A. Neri, M. Todesco, and G. Macedonio (2002), Pyroclastic flow hazard assessment at Vesuvius (Italy) by using numerical modeling. II. Analysis of flow variables, *Bull. Volcanol.*, *64*, 178–191, doi:10.1007/s00445-0010190-1.

Fournier d'Albe, E. M. (1979), Objectives of volcanic monitoring and prediction, *J. Geol. Soc. London*, *136*, 321–326.

Frondini, F., G. Chiodini, S. Calirò, C. Cardellini, D. Granieri, and G. Ventura (2004), Diffuse CO_2 degassing at Vesuvio, *Italy, Bull. Volcanol.*, in press.

Gelman, A., J. B. Carlin, H. S. Stern, and D. B. Rubin (1995), *Bayesian Data Analysis*, Chapman and Hall, New York.

Gigante, M. (1991), Lettere di Plinio il Giovane sull'eruzione vesuviana del 79, in *Un viaggio al Vesuvio*, edited by P. Gasparini and G. Musella, pp. 159–161, Liguori, Naples, Italy.

Granieri, D., G. Chiodini, W. Marzocchi, and R. Avino (2003), Continuous monitoring of CO_2 soil diffuse degassing at Phlegraean Fields: Influence of environmental and volcanic parameters, *Earth Planet. Sci. Lett.*, *212*, 167–179.

Gusev, A. A., V. V. Ponomareva, O. A. Braitseva, I. V. Melekestsev, and L. D. Sulerzhitsky (2003), Great explosive eruptions on Kamchatka during the last 10,000 years: Self-similar irregularity of the output of volcanic products, *J. Geophys. Res.*, *108*(B2), 2126, doi:10.1029/2001JB000312.

Hill, D. P., et al. (2001), Response plan for volcano hazards in the Long Valley Caldera and Mono craters region California, *U.S. Geol. Surv. Bull.*, *2185*, 65 pp.

Kanamori, H. (1980), The state of stress in the Earth's lithosphere, in *Physics of the Earth's Interior*, edited by A. M. Dziewonski and E. Boschi, *Proc. Int. Sch. Phys. Enrico Fermi*, *78*, 531–553.

Kilburn, C. R. J. (2003), Multiscale fracturing as a key to forecasting volcanic eruptions, *J. Volcanol. Geotherm. Res.*, *125*, 271–289.

Lipman, P. W., and D. R. Mullineaux (1981), The 1980 eruptions of Mount St. Helens, Washington, *U.S. Geol. Surv. Prof.*, *1250*.

Lirer, L., P. Petrosino, I. Alberico, and I. Postiglione (2001), Long-term volcanic hazard forecasts based on Somma-Vesuvio past eruptive activity, *Bull. Volcanol.*, *63*, 45–60, doi:10.1007/s004450000121.

McNutt, S. R. (2000)., Volcano seismicity, in *Encyclopedia of Volcanoes*, edited by H. Sigurdsson et al., pp. 1015–1033, Academic, San Diego, Calif.

Nazzaro, A. (1998), Some considerations on the state of Vesuvius in the middle ages and the precursors of 1631 eruption, *Ann. Geophys.*, *41*, 555–565.

Neuberg, J. (2000), Characteristics and causes of shallow seismicity in andesite volcanoes, *Philos. Trans. R. Soc. London*, *358*, 1533–1546.

Newhall, C. G. (2003), "Restless" isn't always dangerous and "quiet" isn't always reassuring!, paper presented at Cities on Volcanoes 3, Univ. of Hawaii, Hilo, 14–18 July .

Newhall, C. G., and R. P. Hoblitt (2002), Constructing event trees for volcanic crises, *Bull. Volcanol.*, *64*, 3–20, doi:10.1007/s004450100173.

Newhall, C. G., and R. S. Punongbayan (1996), *Eruptions and lahars of Mount Pinatubo, Philippines*, Univ. of Wash. Press, Seattle.

Newhall, C. G., and S. Self (1982), The volcanic explosivity index (VEI): An estimate of the explosive magnitude for historical eruptions, *J. Geophys. Res.*, *87*, 1231–1238.

Newhall, C. G., R. S. Punongbayan, and T. M. Gerlach (1994), Tight and leaky volcanoes: Implications for forecasting explosive eruptions, in *Large Explosive Eruptions*, *Atti Conv. Lincei*, vol. 112, pp. 13–21, Accad. Naz. dei Lincei, Rome.

Quareni, F., and F. Mulargia (1993), Modeling of closure of volcanic conduits with an application to Mount Vesuvius, *J. Geophys. Res.*, *98*, 4221–4229.

Recupito, G. C. (1632), *De Vesuviano Incendio Nuntius*, 119 pp., Longo, Naples, Italy.

Romano, C., D. Giordano, P. Papale, V. Mincione, D. B. Dingwell, and M. Rosi (2003), The dry and hydrous viscosities of alkaline melts from Vesuvius and Phlegraean Fields, *Chem. Geol.*, *202*, 23–38.

Sandri, L., W. Marzocchi, and L. Zaccarelli (2003), A new perspective in identifying the precursory patterns of volcanic eruptions, *Bull Volcanol.*, doi:10.1007/s00445-003-0309-7.

Santacroce, R. (1983), A general model for the behavior of the Somma-Vesuvius volcanic complex, *J. Volcanol. Geotherm. Res.*, *17*, 237–248.

Scandone, R., G. Arganese, and F. Galdi (1993a), The evaluation of volcanic risk in the Vesuvian area, *J. Volcanol. Geotherm. Res.*, *58*, 263–271.

Scandone, R., L. Giacomelli, and P. Gasparini (1993b), Mount Vesuvius: 2000 years of volcanological observations, *J. Volcanol. Geotherm. Res.*, *58*, 5–25.

Simkin, T., and L. Siebert (1994), *Volcanoes of the World*, Geosciences, Tucson, Ariz.

Sparks, R. S. J. (2003), Frontiers: Forecasting volcanic eruptions, *Earth Planet. Sci. Lett.*, *210*, 1–15.

UNESCO (1972), Report of consultative meeting of experts on statistical study of natural hazards and their consequences, *Doc. SC/WS/500*, 11 pp., New York.

Voight, B., and R. R. Cornelius (1991), Prospects for eruption prediction in near real-time, *Nature*, *350*, 695–698.

Woo, G. (1999), *The Mathematics of Natural Catastrophes*, 292 pp., Imp. Coll. Press, London.

Zollo, A., W. Marzocchi, P. Capuano, A. Lomax, and G. Iannaccone (2002), Space and time behavior of seismic activity at Mt. Vesuvius volcano, southern Italy, *Bull. Seismol. Soc. Am.*, *92*, 625–640.

E. Boschi, INGV-Roma, Via di Vigna Murata 605, I-00143 Rome, Italy. (presidente@ingv.it)

P. Gasparini, Dipartimento di Fisica, Universita di Napoli "Federico II", Complesso Universitario di Monte S.Angelo, Via Cinthya, I-80126 Naples, Italy. (paolo.gasparini@na.infn.it)

W. Marzocchi and L. Sandri, INGV-Bologna, Via D. Creti 12, I-40128 Bologna, Italy. (marzocchi@bo.ingv.it; sandri@bo.ingv.it)

C. Newhall, USGS, Box 351310, University of Washington, Seattle, WA 98195, USA. (cnewhall@ess.washington.edu)